VOL. 5 No. 2 FEBRUARY 1940

Philips Technical Review

DEALING WITH TECHNICAL PROBLEMS
RELATING TO THE PRODUCTS, PROCESSES AND INVESTIGATIONS OF
N.V. PHILIPS' GLOEILAMPENFABRIEKEN

EDITED BY THE RESEARCH LABORATORY OF N.V. PHILIPS' GLOEILAMPENFABRIEKEN, EINDHOVEN, HOLLAND

THE USE OF MODERN STEELS FOR PERMANENT MAGNETS

by A. TH. van URK.

In order to obtain a certain magnetic field strength in a given air gap with as little magnet steel as possible, the construction of the magnet must be so chosen that the product of induction and field strength in the interior of the magnet steel is as large as possible. In the case of modern magnet steels with very high coercive force and relatively low residual magnetism, this condition leads to quite different constructions than in the case of the older kinds of steel with low coercive force and high residual magnetism. It is explained in this article how one sets about the construction of a magnet. In the first part spreading is neglected: in the second part a semi-empirical method is given of taking spreading into account.

Introduction

If we wish to improve upon a magnet made of the tungsten steel [1]) formerly used, it would seem obvious simply to substitute for the tungsten steel a piece of modern magnet steel of the same shape. The result would, however, usually be found very disappointing: the magnet is scarcely improved at all. The modern magnet steel may even produce a weaker field than tungsten steel.

On the other hand it has been found that upon judicious construction of the whole magnet modern magnet steels do give very much better results than the steels formerly used, and that with the magnet steel "Ticonal 2A" for instance a field can be excited in a given air gap which could only be obtained with ten times as much tungsten steel. It follows from this that the disappointment mentioned above must not be ascribed to the steel itself, but to the fact that a design intended for tungsten steel is not suitable for making the most of the specific qualities of the modern magnet steels.

The aim of this article is to find out the reason for this, and to learn how a magnet should be designed in order to use a given kind of magnet steel to the greatest advantage.

[1]) Tungsten steel may be considered as the best representative of the older type of magnet steel. Modern magnet steels differ in physical respects from the steels used earlier mainly in the nature of the rearrangement processes in the material by which the magnetic hardness is obtained; see in this connection: J. L. Snoek, Philips techn. Rev. 2, 233, 1937.

Comparison of modern and older kinds of steel

The properties of a magnet steel are determined by its magnetization curve. The shape of this curve can be established approximately by the values of residual magnetism and coercive force (see *fig. 1*). The residual magnetism or remanence is the maximum induction which remains in the steel when the magnetizing field is reduced to zero after the steel has been magnetized to saturation. The coercive force is the magnetic field which must be applied in a direction opposite to the residual induction in order to reduce the latter to zero.

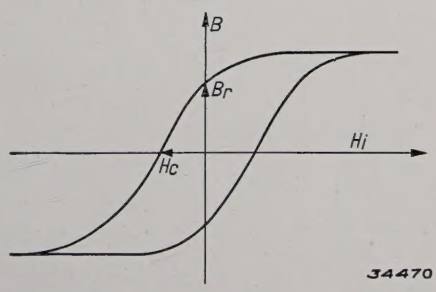

Fig. 1. Induction B of a magnet steel as a function of the internal field H_i. The remanence is B_r, the coercive force H_c.

Fig. 2 gives the magnetization curve of a modern nickel- aluminium steel, such for example as the previously mentioned "Ticonal 2A", compared with that of a tungsten steel. It may be seen that an increase of the coercive force of nearly tenfold is obtained by the sacrifice of part of the remanence, which has fallen back to nearly one half. In spite

of its lower remanence, however, the magnet steel "Ticonal" must in general be considered very much better than tungsten steel. In order to show why this is so, we shall examine the results obtained in solution of the problem of obtaining a certain field strength in a given air gap with as little magnet steel as possible.

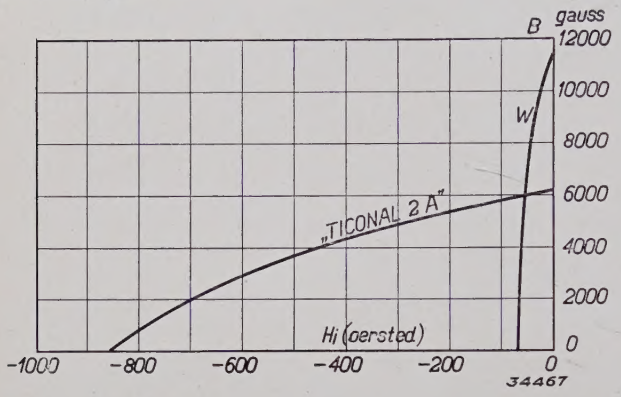

Fig. 2. Induction B of a tungsten steel (W) and of the magnet steel "Ticonal 2A", as functions of the internal field H_i which is opposite in direction to the induction in the part of the curve given.

Simplified calculation of a magnet

We shall begin with a magnet constructed as indicated in *fig. 3*, namely a magnet of length L and cross section S, upon which two pieces of soft iron are fastened, which together bound an air gap of length l and cross section s. For the sake of simplification we shall assume for the present that the lines of force of the magnet must all pass through the air gap in order to pass from the north to the south pole. Thus spreading is neglected. Furthermore, the fields in the magnet steel and in the air gap will be considered homogeneous, and we shall also assume that the soft iron is absolutely conductive for magnetic flux, *i.e.* at any arbitrary value of the induction B the field H_i in the soft iron is zero.

The magnetic condition of the model thus simplified can be described by three quantities: the external field strength H in the air gap, the internal field strength H_i and the induction B of the magnet

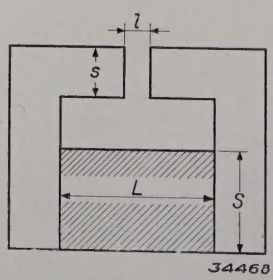

Fig. 3. Model for simplified calculation of a magnet. The air gap has a length l and a cross-section area of s; the magnet steel has a length L and a cross-section area S.

steel. Now three equations are sufficient for the calculation of a magnet in the first approximation.

The first equation is derived from the proposition that the total magnetic flux is the same through every cross section of the system, and therefore also through a cross section of the magnet and of the air gap. The equation is therefore as follows:

$$B\,S = H\,s. \quad \ldots\ldots\ldots \quad (1)$$

The second equation follows from the proposition that the line integral of the magnetic field strength is zero along every closed path. Since the field strength is assumed to be zero in the soft iron, this means that:

$$H\,l + H_i\,L = 0, \quad \ldots\ldots \quad (2)$$

$$H_i\,L = -\,H\,l. \quad \ldots\ldots\ldots \quad (2a)$$

H_i is therefore opposite in sign (opposite in direction) to H.

Finally as third equation we have the relation between B and H_i which is given by the magnetization curve of the magnet steel:

$$B = f\,(H_i) \quad \ldots\ldots\ldots \quad (3)$$

We are practically concerned with the part of the curve in which the direction of the field strength is opposite to that of the induction (*cf.* fig. 2), so that the field has a demagnetizing action. Before we make use of this curve, we shall however first draw a general conclusion which becomes obvious when we multiply equations (1) and (2*a*) by each other. The result of this operation:

$$-\,B\,H_i\,L\,S = H^2\,l\,s \quad \ldots \quad (4)$$

expresses the fact that the volume l_s of the air gap, multiplied by the square of the field strength, is equal to the volume LS of the magnet, multiplied by the absolute value of the product BH_i. Since the problem is, with a given air gap and field strength in the air gap, *i.e.* with a given second term, to keep the volume LS of the magnet as small as possible, it follows from (4) that we must choose a magnet steel or a design of construction whereby the product BH_i is as large as possible. Now for a given magnet steel BH_i is not a constant, but depends upon the value of H_i. That is obvious, because the product disappears for $H_i = 0$ (B is equal to the remanence), as well as for $B = 0$ (H_i is equal to the coercive force), while at intermediate values it is not equal to zero. With a given value of H_i, therefore, the product will have a maximum (see *fig. 4*).

The height of the maximum of $B H_i$ now provides us with a measure of the quality of a magnet steel, while the corresponding value of H_i determines the most favourable design of the magnet. For tungsten steel the maximum lies at 30 oersted and amounts to 2×10^5 gauss-oersted; for "Ticonal 2A" the maximum lies at 400 oersted and amounts to 1.8×10^6 gauss-oersted. According to equation (4), therefore, nine times less "Ticonal" steel than tungsten steel is necessary to produce the same field in a given air gap.

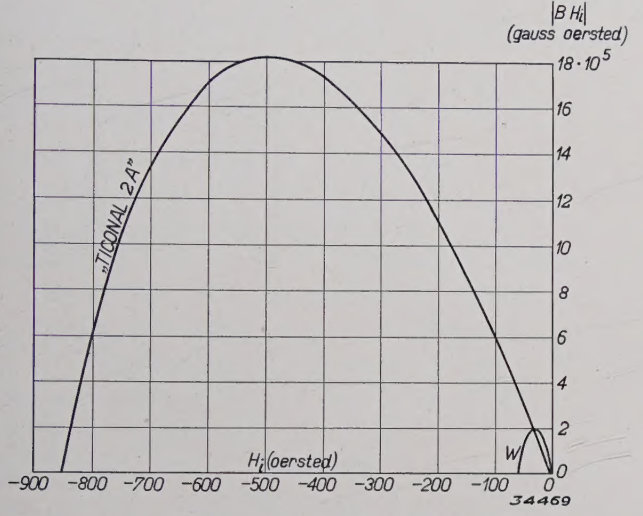

Fig. 4. Absolute value of the product BH_i (induction times internal field) as a function of H_i for a tungsten steel (W) and for the magnet steel "Ticonal 2A".

After we have calculated the volume of magnet steel needed, we can calculate the required length of the magnet with the help of equation (2). We find

$$L = -\frac{H}{H_i} l \quad \ldots\ldots\ldots \quad (5)$$

and we must substitute here for H_i the optimum value (with "Ticonal" 400 oersted). The cross section of the magnet is now of course also known. The following relation is valid, according to equation (1):

$$S = \frac{Hs}{B}, \quad \ldots\ldots\ldots \quad (6)$$

where B is the induction which, according to equation (3), corresponds to the optimum value of the demagnetizing field H_i.

From equations (5) and (6) it is clear how the design of a magnet must be changed when a tungsten steel is replaced by "Ticonal". The optimum field H_i has increased thirteen times and according to equation (5) this means that the length of a "Ticonal" magnet must be only $^1/_{13}$ of that of a tungsten steel magnet which produces the same field. On the other hand the induction B for optimum field strength in the case of the magnet steel "Ticonal" is slightly lower than with a tungsten steel; according to equation (6), therefore, the cross section S must be taken slightly larger.

We are now also able to understand why the replacing of a tungsten steel by the magnet steel "Ticonal" (without alteration in design) does not always lead to a better result. To show this we divide equation (1) by (2a):

$$\frac{B}{H_i} = -\frac{L}{S}\frac{s}{l} \quad \ldots\ldots\ldots \quad (7)$$

Thus if we have a magnet and an air gap of known dimensions, the ratio B/H_i is known. In the diagram of the magnetization curve this gives us a straight line through the origin which cuts the magnetization curve at a point which gives us the values of B and H_i. Now it is quite possible (see *fig. 5*) for this line to cut the curve of the better steel at a point which gives a lower product of BH_i than the point at which it cuts the curve for the poorer steel. It is, however, clear that in this case the magnet of the better steel is very badly proportioned. By changing the design it is certainly possible to obtain a considerably better result with the same quantity of magnet steel.

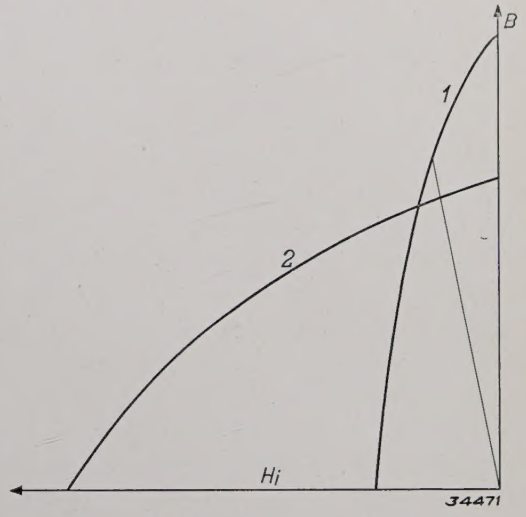

Fig. 5. The ratio between the induction B and the internal field H_i with a given design is independent of the properties of the magnet steel. With a sufficiently high value of this ratio (slope of the straight line B/H_i = constant) the product BH_i is greater for the magnet steel *1* than for the steel *2*, although the maximum value of the product is smaller for steel *1* than for steel *2*.

The spreading of lines of force

Until now we have failed to take into account the spreading of the lines of force. We reached the conclusion that the quality of a magnet steel is

determined solely by the maximum value of the product BH_i. A lowering of the remanence of the magnet steel therefore meets with no objections, if only it is accompanied by a corresponding increase in the coercive force. Such a change in the magnetic properties has, however, the result that the design must be altered, and the new design may have considerably more spreading than the old. An example will serve to illustrate this point.

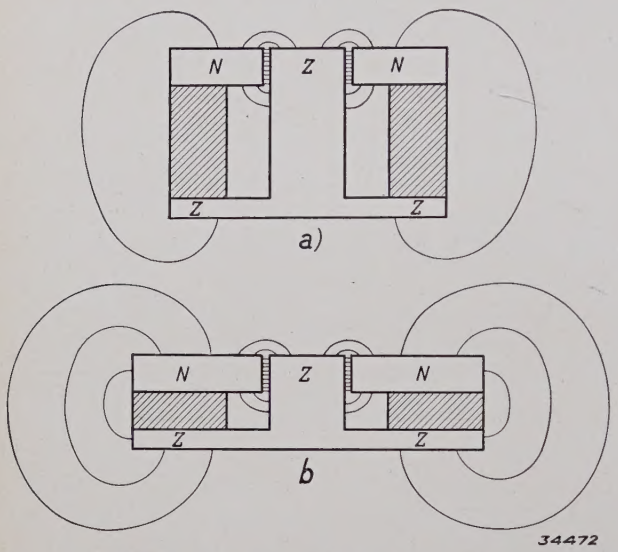

Fig. 6. a) Diagram of a cross section of a loud speaker magnet, constructed of the magnet steel "Ticonal 2A". b) Cross section of the same magnet, if the coercive force of the steel were three times as great, and the remanence one third. The shape changes in such a way that the spreading becomes considerably greater.

Fig. 6a shows the cross section of a magnet such as is used in loud speakers. The magnet steel is shaded, while the soft iron of the pole pieces is left white. The relative dimensions of this magnet are adapted to the *B-H* curve of the magnet steel "Ticonal 2A". If a tungsten steel were used, the height of the magnet would have to be considerably greater, while the diameter could be taken slightly smaller.

Let us now consider the imaginary case where, while the product BH_i is kept constant, the coercive force of the steel is three times as great as that of "Ticonal", while the remanence is only one third of that of "Ticonal". The magnet would then have the shape given in fig. 6*b*. As far as spreading is concerned, the design is much less satisfactory. In the first place, due to the increase in diameter, the surface from which the spread field originates is increased, and in the second place, due to the decrease in height, the resistance of the air path for the lines of force of the spread field is considerably decreased. Although when spreading is disregarded the second magnet steel is just as good as the first, it will not be possible to obtain as good results with it when it is used as a loud speaker magnet. It may be stated as a general conclusion, that the question as to which magnet steel is the most suitable for exciting a field of a certain strength in an air gap of a given form, cannot be answered by noting exclusively the maximum value of BH_i, but that B and H_i themselves also play a part. In particular the remanence of the magnet steel "Ticonal 2A" is found to be too low for certain applications. A new magnet steel has therefore been developed which has a slightly lower coercive force than "Ticonal 2A", but practically twice its remanence, namely 12 000 gauss. The maximum value of BH_i in the case of this steel is also twice as great. In *fig. 7* may be seen the magnetization curve of this magnet steel which has been called "Ticonal 3.8".

If we now return to the question of how a magnet must be constructed in order to use the magnet steel to the greatest possible advantage, our qualitative considerations of the influence of spreading are inadequate, and must be supplemented by a method of taking the spreading into account quantitatively in the calculation of the magnet.

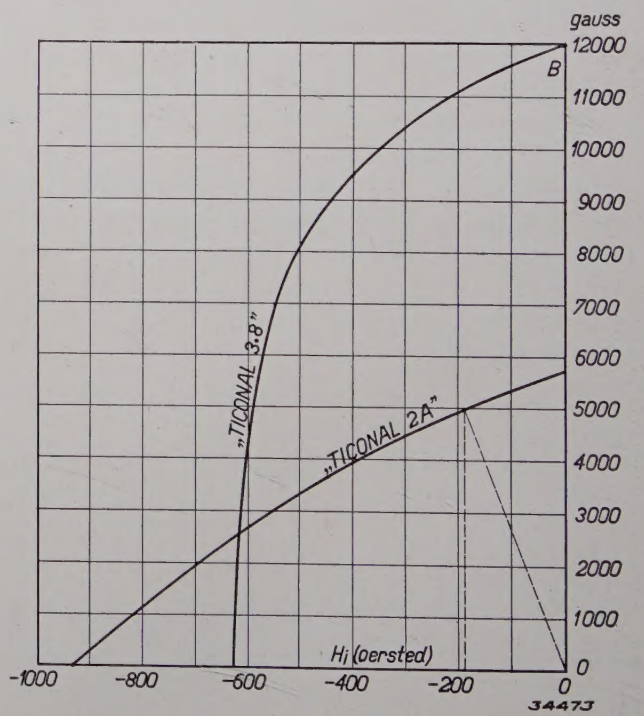

Fig. 7. Magnetization curve of the magnet steel "Ticonal 3.8", compared with that of "Ticonal 2A". The dotted lines refer to the examples treated in the conclusion.

More precise calculation of a magnet

The more elaborate calculation of a magnet which we shall carry out in the following differs from the above simplified treatment in the fact

that we determine not only the flux in the effective air gap, but the flux between each pair of surfaces between which lines of force pass through the air.

In calculating these different components of the total flux we can to our advantage make use of the concept of "magnetic potential", which is defined in the following way:

$$U_M = \int_{P_0}^{P} H_s \, ds,$$

where ds represents an element of a line drawn from a point P_0, at which the magnetic potential is considered to be zero, to the point P, at which the magnetic potential is indicated by the integral. H_s is the component of H in the direction of the line element ds.

The flux for each two surfaces between which lines of force pass can now be represented by the magnetic potential difference, multiplied by the magnetic conductivity. The latter quantity is therefore defined in exactly the same way as an electrical conductivity. The magnetic conductivity of a rod of length l, cross section s and permeability μ is:

$$g = \mu s/l \, .$$

The specific conductivity is thus nothing else than the permeability.

The conductivity of the air path between two surfaces is equal to the cross section of the bundle of lines of force which pass between the two surfaces. Actually both the cross section and the length must be considered as some kind of average values. The way in which these average values are determined will be discussed presently on the basis of an example.

If U_k is the potential difference between every pair of surfaces and g_k is the corresponding conductivity, the total flux

$$\Phi = \Sigma \, U_k \, g_k \, . \quad . \quad . \quad . \quad . \quad . \quad . \quad (8)$$

The total flux Φ is often compared with the effective flux $\Phi_0 = U_0 \, g_0$ which passes through the air gap. The ratio Φ/Φ_0 is called the coefficient of spreading σ.

When the coefficient of spreading is known, the calculation of the magnet can be carried out in the way discussed at the beginning of this paper. Equation (1) must be replaced by the more precise relation

$$B \, S = H \, s \, \sigma \, . \quad . \quad . \quad . \quad . \quad . \quad (9)$$

and this, together with equations (2) and (3) gives the three unknowns B, H_i and H.

The whole problem is thus reduced to the measurement or calculation of the terms $U_k \, g_k$ or $U_0 \, g_0$, which appear in the calculation of the coefficient of spreading σ. Often there is appreciable spreading only between the soft iron pole pieces, between which the air gap is situated. The different magnetic potential differences U_k are then practically equal to each other and to U_M. In that case only the conductivities g_k or g_0 occur in equation (8).

The conductivities can be calculated exactly in certain simple configurations. Usually, however, the calculation is very difficult or even impossible. Since this problem has great practical significance, for instance for the construction of measuring instruments, we shall explain in the following how formulae can be arrived at by a semi-empirical method which make it possible to calculate the field in the air gap of a magnet for different shapes and sizes of the magnet and different kinds of magnet steel.

As cross section of the bundle of lines of force which pass between two surfaces, we take the average size of the two surfaces. In order to determine the length of path in the air, we choose a simple shape for the lines of force, a straight line or part of a circle, for instance. The formula for the conductivity so obtained is finally completed by a numerical factor which is determined experimentally by measuring on a model the flux which passes between these two surfaces. It is clear that with the help of the formulae so obtained it is only possible to make precise calculations for a model which is an enlarged or reduced reproduction of the experimental model. The great value of the method, however, lies in the fact that the empirically found numerical factors apparently do not change when the relations between the various dimensions of the magnet and the nature of the magnet steel in the actual practical model are quite different from those of the experimental model. With the help of the same formula, therefore, it is possible to anticipate the properties of very different types of magnets. A simple example will be given in the following.

Complete calculation of a simple example

As example we have chosen the design represented in *fig. 8*, which consists of two cylindrical magnets M lying in a straight line, provided with iron pole pieces P and closed by an iron armature B which is thick enough to have practically no magnetic resistance. The distance a between the armature and the pole pieces is made so great that practically no appreciable flux will pass across this air space.

Let us assume that the left-hand pole piece is the north pole and the right-hand one the south pole. The flux through the air space can be divided as follows:

1) the flux Φ_1 from the left-hand magnet to the right-hand magnet;
2) the flux Φ_2 from the wall of the cylinder of the left-hand pole piece to that of the right-hand pole piece;
3) the effective flux Φ_3 from the flat surface of the left-hand pole piece to that of the right-hand pole piece.

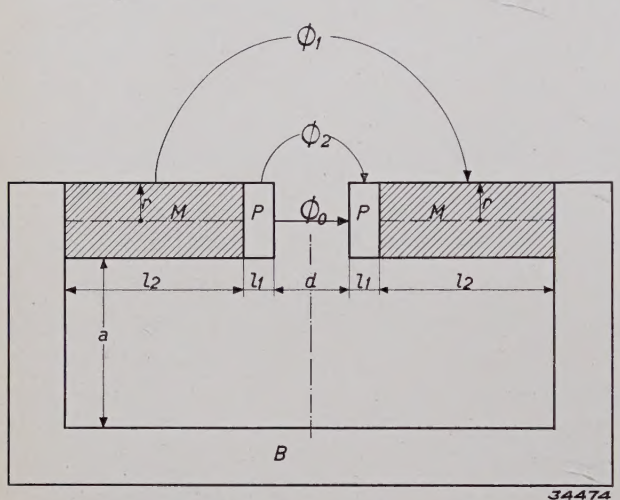

Fig. 8. Model of a magnet whose effective flux Φ_0 and spread flux $\Phi_1 + \Phi_2$ can be calculated by a semi-empirical method. Cross hatched: magnet steel, white: soft iron.

The flux Φ_1 will be proportional to the cylindrical surface $2\,\pi\,r\,l_2$ of the magnet, and inversely proportional to the length of the lines of force. For this latter length we take as average value the length of the semicircle drawn in the figure, which is equal to

$$\pi\left(\frac{d}{2} + l_1 + \frac{l_2}{2}\right).$$

The magnetic potential then passes from the value 0 for the outermost line of force to the value $2\,l_2\,H_i$ for the innermost one; we have here taken as average value $l_2\,H_i$. In this way we arrive at the formula:

$$\Phi_1 = \alpha\,\frac{2\,\pi\,r\,l_2}{\pi\left(\frac{d}{2} + l_1 + \frac{l_2}{2}\right)}\,H_i\,l_2 = \alpha\,\frac{4\,r\,l_2^2}{d + 2\,l_1 + l_2}\,H_i \quad . \quad (10)$$

It will be seen that in addition to the quantities already mentioned another factor α has been introduced. This factor is determined experimentally by measuring the flux Φ_1. The formula is in this way made to produce the correct result for a given model. In general it is found that the empirical correction factor does not change very much when one passes from the experimental model to a design with quite different dimensions, r, l_1, l_2, d; this is the basis of the whole method of calculation.

The flux Φ_2 through the side wall of the soft iron pole piece is calculated in exactly the same way as the flux Φ_1; the result is:

$$\Phi_2 = \beta\,\frac{2\,\pi\,r\,l_1}{\pi\left(\frac{d_1}{2} + \frac{l_1}{2}\right)}\,2\,H_i\,l_2 = \beta\,\frac{8\,r\,l_1\,l_2}{d + l_1}\,H_i, \quad . \quad (11)$$

where β is again a factor which must be determined experimentally.

Finally we calculate the effective flux. The length of the lines of force (d) and the cross section of the bundle of lines of force ($\pi\,r^2$) are well defined with a sufficiently narrow air gap, so that it is unnecessary to introduce a correction factor. The following result is obtained:

$$\Phi_0 = \frac{\pi r^2}{d}\,2\,H_i\,l^2 \quad . \quad . \quad . \quad . \quad . \quad (12)$$

The experiments for the determination of α and β were carried out with a magnet of "Ticonal 3.8" having the dimensions:

$r = 1.28$ cm,
$d = 0.515$ cm,
$l_1 = 0.2$ cm,
$l_2 = 3$ cm.

The following values were found:

$H = 4\,300$ oersted,
$\Phi_1 = 15\,100$ maxwell,
$\Phi_2 = 13\,300$ „ ,
$\Phi_0 = 22\,400$ „ ,
total flux $\Phi = 50\,800$ „ ,
$\sigma = \Phi/\Phi_0 = 2.27.$

From the measured value of Φ_0, with the help of equation (12) we can calculate the internal field H_i, and we find a value of 373 oersted. By means of equation (9) and (10) the spread flux Φ_1 and Φ_2 can now be calculated. The results are:

$\Phi_1 = \alpha \cdot 4\,400$ maxwell,
$\Phi_2 = \beta \cdot 3\,100$ „ .

By comparing these values with the measured values of Φ_1 and Φ_2 we find:

$$\alpha = 3.43$$
$$\beta = 4.14.\ ^{2})$$

All the quantities are now known which are necessary for setting up a formula for the coefficient of spreading with the help of equations (9), (10), (11) and (12):

$$\sigma = (\Phi_1 + \Phi_2 + \Phi_0)/\Phi_0 =$$
$$= \frac{2\,d}{\pi\,r}\left(\frac{3{,}43\,l_2}{d + 2l_1 + l_2} + \frac{8{,}28\,l_1}{d + l_1}\right) + 1. \quad (13)$$

Equation (13) forms the basis for the calculation of a magnet of the type described above. If the coefficient of spreading σ is known, equations (2), (3) and (9) give us the other unknowns, H, H_i and B.

In order to check the formula and thus to test the whole method, a second model was made with very different dimensions from those of the test model, while in addition a different kind of magnet steel "Ticonal 2A" was used instead of "Ticonal 3.8" (see fig. 7). The dimensions of the second model are the following:

$$r = 1.7 \text{ cm},$$
$$d = 2.05 \text{ cm},$$
$$l_1 = 1.0 \text{ cm},$$
$$l_2 = 5.6 \text{ cm},$$

cross section magnet [3]) 8.28 cm^2.

The field H in the air gap of this magnet was found to be 980 oersted. Let us now find the field strength which is to be expected on the basis of the formulae derived above.

According to (13) we find

$$\sigma = 4.6.$$

According to equation (9) $8.28\,B = H \times 9.08 \times 4.6$, while according to equation (2)

$$H_i = -\,H\,\frac{2{,}05}{11{,}2}\,.$$

If we eliminate H from these two equations (as was done in the derivation of equation (7)), it follows that:

$$\frac{B}{H_i} = \frac{9{,}08 \cdot 4{,}6 \cdot 11{,}2}{2{,}05 \cdot 8{,}28} = 27{,}6.$$

Now with the help of the magnetization curve we can also determine B and H_i themselves: the line $B/H_i = 27.6$ cuts the B-H_i curve of the magnet steel used ("Ticonal 2A") at the point

$$B = 5\,000 \text{ gauss}, \quad H_i = -182 \text{ oersted}.$$

We finally find for the field in the air gap

$$H = \frac{-11{,}2}{2{,}05}\,H_i = 994 \text{ oersted}.$$

The discrepancy with the measured result thus amounts to only 1·5 per cent, which must be considered fairly satisfactory, especially when it is kept in mind that the control model had quite different dimensions from the test model (the ratio between the spread flux and the effective flux is, for example, three times a great as in the test model).

Having seen how a magnet can be calculated, it remains to find out how a magnet can be designed in order to provide a given field in a given air gap. We begin by calculating the length and the cross-sectional area of the magnet steel according to the equations (2a) and (9). For H_i we choose a favourable value, and estimate the value of the coefficient of spreading σ. With the dimensions of the steel obtained we design a magnet and then calculate σ according to equation (13). If the calculated value agrees with the estimated one, the work is finished, otherwise we repeat the calculation with the new value of σ and the result will be attained after a second or third attempt.

---

[2]) α and β are much larger than one, which means that our estimation of the conductivity before the introduction of the correction factor was very inaccurate. The fact that the actual conductivity is very much higher is understandable. The area of the cross section of the bundle is very much greater at the middle than we have assumed. It is remarkable that this rough method of taking spreading into account gives fairly good results in the end.

[3]) The magnet had a hole along the axis so that its cross-section area was slightly less than $\pi\,r^2$.

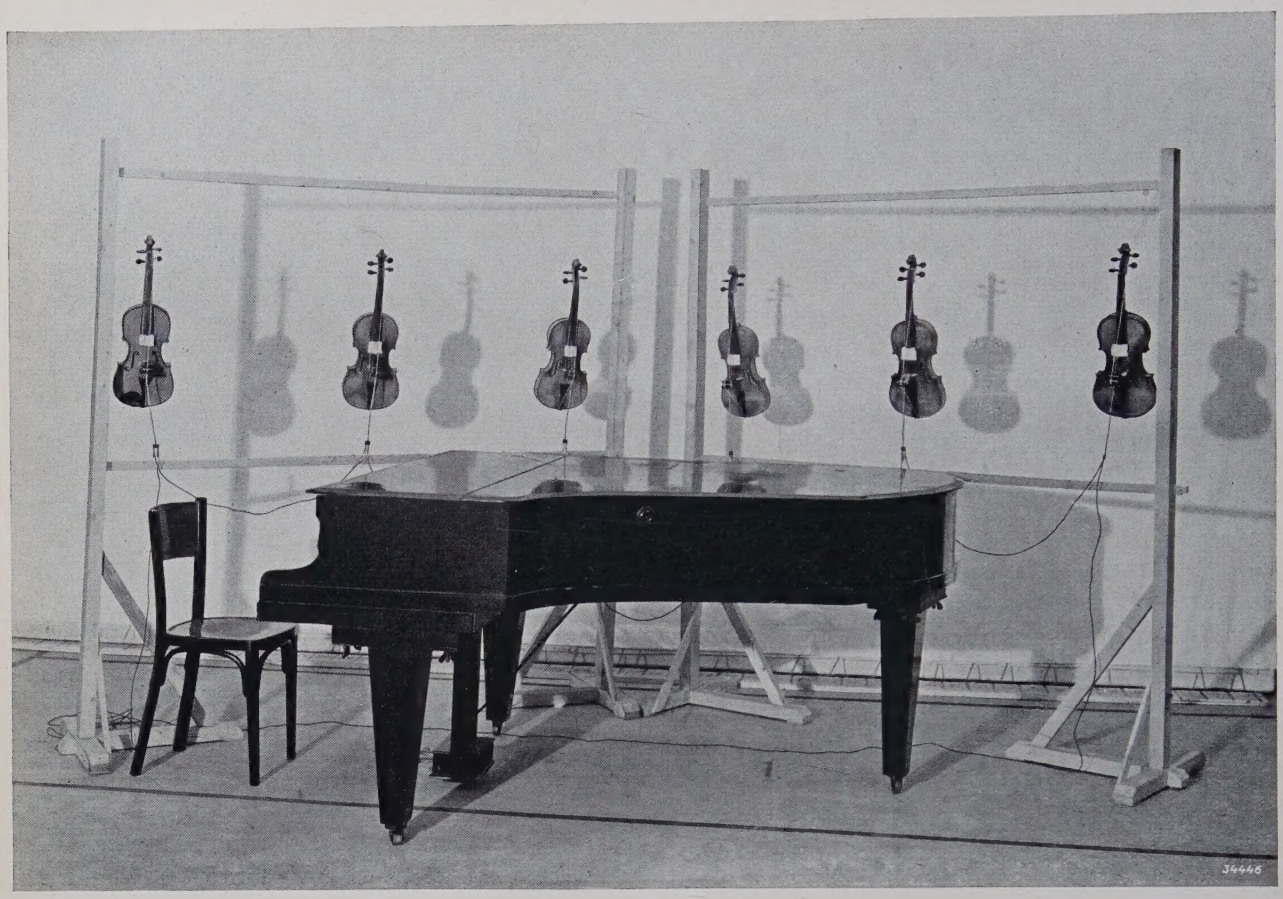

PERSPECTIVES IN THE DEVELOPMENT OF THE VIOLIN

by R. VERMEULEN.

534.86: 787.1

A discussion is given of a method of obtaining sufficient amplification of the sound of a solo violin with respect to the accompanying orchestra. The arrangement tested in the Philips Laboratory is described and various factors are discussed which would be of importance in its practical application.

In reading the title of this article one will probably be tempted to ask immediately: "Does the need of further development of the violin exist? Is not the situation rather that violin builders would like nothing better than to return to the standard already reached by Stradivarius and Guarnerius in the eighteenth century?"

Nevertheless it is not unreasonable to speak of a need of development for the violin. This need has arisen simply due to the fact that the purposes for which the violin is used have changed with time. While in the beginning — we are thinking of the sixteenth century, since which time no further fundamental changes in the construction of the violin have occurred — the violin was used chiefly for chamber music and for musical programmes in the reverberating spaces of churches, the present day practice of music makes it necessary that the violin be played in concert halls often of enormous size, and before huge audiences. This practice makes much higher demands on the volume of sound which must be produced by the source. These demands are reflected clearly in the greatly increased size of orchestra: each instrumental voice occurring in the score is played by a group of representatives in unison; each violin voice is played by a large number of violins, as many as 25, for example.

This method of increasing the intensity, namely by the multiplication of the number of musicians, gives no difficulty as long as nothing more than average skill upon his instrument is demanded of each collaborator. The situation, however, is quite different when it is a question of musicians of exceptional talent who appear as soloists, for instance in a violin concert with orchestral accompaniment. The soloist must then play against the whole orchestra with his single violin, and even though

the conductor imposes the greatest restraint on the orchestra, it often becomes a "concert" in the truest sense of the word, a "competition", in which it costs the soloist the greatest effort to bring out his instrument sufficiently strongly above the accompaniment. It is obvious that this is not exactly desirable. There is not only the danger that the artist will be distracted by the exertion from complete surrender to the music he is interpreting, but moreover the quality of the tone may suffer because of the fact that non-linear distortion may occur with too great amplitudes of the strings and sounding boards, and result in squeaking and scratching. Every violin soloist will acknowledge the fact that it would be an improvement very much to be appreciated if it were possible to increase the volume of sound from the violin while retaining its other qualities.

How could this be done? It is known from experience that the instruments of the above-mentioned famous violin builders of the 18th century not only possess a more beautiful tone, but that they produce a greater intensity with much less effort. The knowledge of the methods used to obtain these qualities seems to have been lost, so that until now we have been unable to equal these old violins. Some people even believe that efforts in this direction are doomed to failure because the old violins owe their fine quality to the fact that they are so old and have been played for so long a time by so many excellent violinists. Aside from this, however, the desired effect could not be achieved even if it were possible to copy the old violins exactly, since even a Stradivarius does not produce enough volume to come out above the accompaniment of a large orchestra.

A second possibility of amplifying the sound of the instrument would be to increase its dimensions. As was explained some time ago in this periodical in connection with the simplest sound radiator, the pulsating sphere [1]), the acoustic power produced increases with the size of the radiator. In our case, however, this method cannot be considered for obvious reasons: the size of a violin determines to a large extent its timbre. If we make it larger we do not obtain a louder violin, but a viola or a cello.

A solution of this difficulty may be sought by making use of modern electro-acoustic aids. The sound of a violin can be picked up with a microphone, the microphone voltage amplified at will and fed to a loud speaker. But the question now arises: where must we place the microphone? It would be most reasonable to pick up the sound of the violin at the position of the hearers. If we do this, however, we are no further ahead, since the sound of the orchestra is then amplified together with the violin solo. In order to shift the ratio of the two sound contributions in favour of the solo instrument the microphone would therefore have to be hung in the immediate neighbourhood of that instrument. Such a solution is employed for example in the analogous case in which a singer's voice must be clearly heard above a jazz band. Placing the microphone close to the source of sound, however, has the objection that the sound may differ considerably in timbre from that at a greater distance. In the example mentioned of the jazz singer this fact has led to the development of a special singing technique known as "crooning". The violin is, however, much larger than the mouth opening of a jazz singer, and moreover, the violinist needs a certain freedom of movement, so that the placing of the microphone close to the solo violin cannot be considered.

These difficulties are avoided if, instead of the acoustic vibrations around the violin, the mechanical vibrations of the body of the violin are picked up [2]) with the help of a kind of electrical gramophone pick-up, and then amplified. The practical realization of this principle, which has been tested in the Philips Laboratory, involves several other considerations which we shall discuss briefly.

When the bow slides over a string a relaxation vibration sets in, in which the deviation of the string varies as a function of the time approximately according to a saw-tooth relation (*fig. 1*).

Fig. 1. The deviation of a bowed violin string as a function of the time. The shadow of a point of the string is photographed during vibration on a constantly moving film (H. Backhaus, Naturwiss. **17**, 811, 1929).

This vibration of the string, which is composed of a large number of harmonics, is communicated *via* the bridge to the body of the violin, which then in turn begins to vibrate and radiates the vibrations in the form of sound. By the very pronounced resonances of the body of the violin (see the frequency characteristic *fig. 2*) harmonics in certain regions are amplified and the typical violin quality

[1]) A. Th. van Urk and R. Vermeulen, Radiation of sound, Philips techn. Rev. **4**, 213, 1939.

[2]) Similar considerations have already been discussed in this periodical in the description of the laringophone which makes telephone communication possible in places where there is much noise: Philips techn. Rev. **4**, 6, 1940.

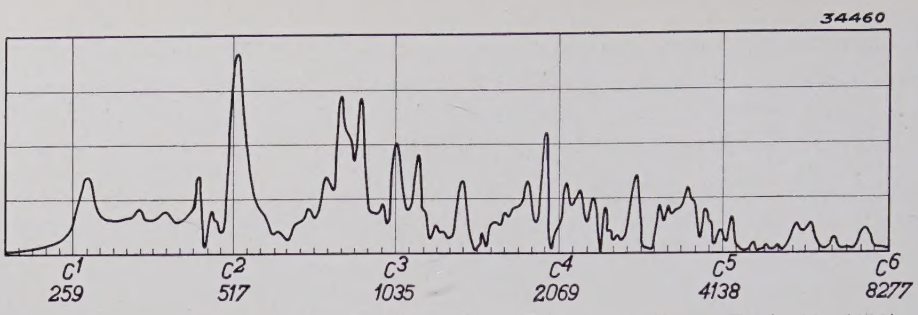

Fig. 2. Frequency characteristic of a violin (from H. Meinel, Akust. Z. 4, 89, 1939).

is obtained: the body of the violin thus determines the timbre. To each of the resonances mentioned there corresponds a certain form of vibration of the body of the violin which could be made visible by Chladni sound figures. From this it follows, however, that it is impossible to use the mechanical vibrations of the body of the violin itself for the purpose in view. If one should set the needle of a vibration pick-up at any point on the sounding board for a given frequency, this point might just lie at a node of the vibration occurring, so that this frequency would not be communicated. The only spot on the whole violin where all the vibrations will certainly be encountered is the bridge, which passes the vibrations of the strings on to the sounding board.

On the other hand we have just seen that the vibrations of the bridge can by no means represent the sound of the violin, since they have not yet passed through the timbre-determining organ. If therefore we should reproduce the vibrations of the bridge by means of an ordinary loud speaker, the sound so obtained would not resemble the sound of a violin. In this way we arrive at the remarkable conclusion that in reproducing the vibrations we must still include the organ which determines the timbre, namely by using a violin body as loud speaker. *The vibrations which are picked up from*

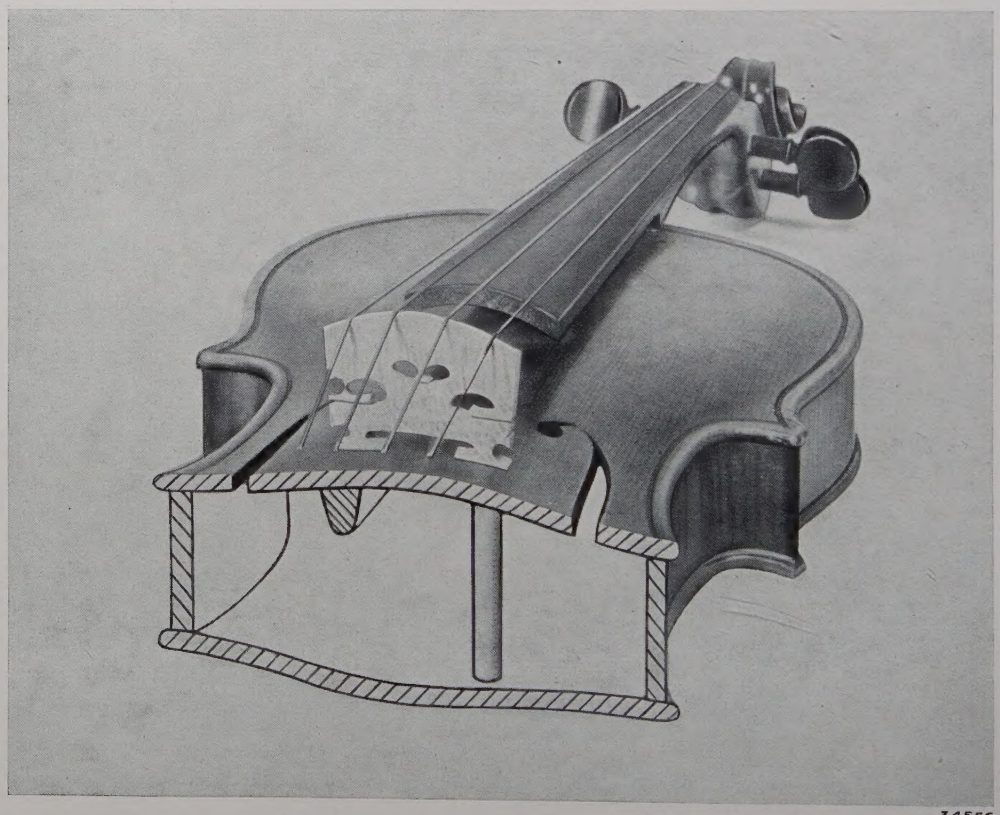

Fig. 3. Cross section through a violin at the position of the bridge. To the right (under the E-string) the sound post, to the left (under the G-string) the bass bar. The strings vibrate chiefly in a horizontal direction.

the bridge of the solo violin are communicated to the bridge of a second violin which then in principle radiates the same sound as if it were made to vibrate by the vibrations of the strings of the first violin [3]).

In picking up the vibrations it is not a matter of indifference what spot on the bridge is chosen. *Fig. 3* shows a cross section of a violin through the bridge. Under the right hand end of the bridge, *i.e.* under the E-string there is a vertical wooden peg between the belly and the back of the violin, the so-called sound post. The amplitude of the belly at this point is therefore practically zero, and we may say that the bridge can only execute a rotating motion about its right hand point of support. The rotating motion of the bridge is caused by the strings vibrating mainly in a horizontal direction. By the left-hand point of support the belly of the violin is then brought into transverse vibration. In order to spread this vibrating motion over a larger surface the sounding board at this point (under the G-string) is reinforced by a thicker oblong piece of wood, the so-called bass bar.

As point of contact for the point of the vibration pick-up with which we wish to amplify the sound of the violin, we choose the spot on the bridge indicated by a circle (*fig. 4*), since we can expect

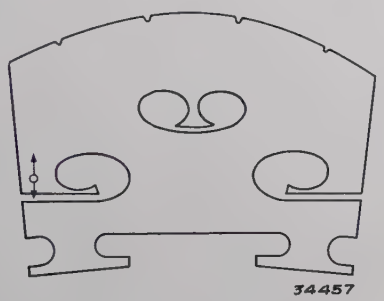

Fig. 4. Bridge of a violin (natural size). Since the bridge executes chiefly a rotating motion around its right-hand point of support, the greatest amplitudes occur on the left. The point of the vibration pick-up is placed on the spot indicated by a circle; it can move in the direction of the arrow.

to find the greatest amplitudes here. The point then moves in the direction of the arrow (perpendicular to the sounding board). *Fig. 5* shows the method of attaching the vibration pick-up, details are described in the text below the figure.

The excitation of the bridge of the "loud speaker violin" is by means of an apparatus similar to that used for the recording of gramophone records which has previously been described in this periodical [4]).

[3]) When loud speaker technology was still in its infancy, a violin or mandolin body was sometimes used as loud speaker. This was done, however, to amplify the normal sound of speech or music. The fact that this was a mistaken idea is clear after the above.

[4]) K. de Boer and A. Th. van Urk, A simple apparatus for sound recording, Philips techn. Rev. **4**, 106, 1939.

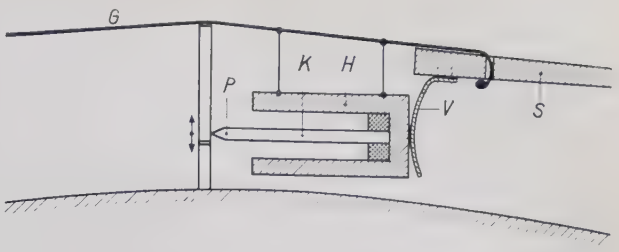

Fig. 5. The vibration pick-up consists of a piëzo-crystal K which is fastened elastically in a holder H and which carries the point P excited by the bridge. The construction and action of this resembles closely that of the crystal laringophone described in the article already cited [2]). The holder H is suspended on the dead end of the G-string G, and is pushed in the direction of the bridge by the spring V which is attached to the tail piece of the violin. When the bridge vibrates the relatively heavy holder H remains practically at rest and the crystal K executes vibrational bending movements upon which a piëzo-voltage occurs between the upper and lower sides of the crystal. This voltage is picked up by means of electrodes stuck to the crystal, and, after amplification, fed to the "loud-speaker violin".

In order to apply the principle entirely consistently the excitation should take place at the spot on the bridge corresponding to that at which the vibrations were picked up on the solo violin. In practice this was not found possible since the spot indicated in fig. 4 is not suitable for the firm attachment of the

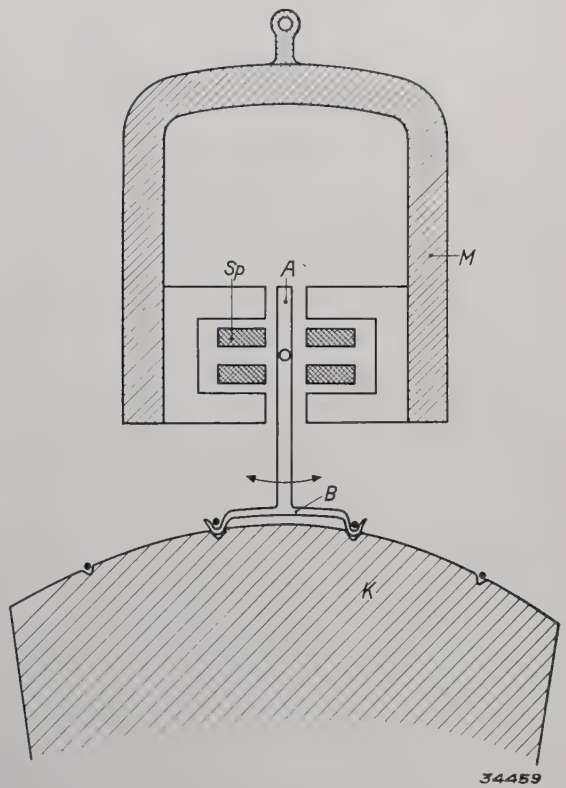

Fig. 6. Excitation of the loud-speaker violin. A bent strip of metal B is set on top of the bridge and held in place by the two middle strings. The metal strip is fastened to the electrically excited armature A, and upon vibration of the armature it exerts a couple in the plane of the bridge. The heavy mass of the magnet M and the pole pieces remain practically at rest. The weight of these parts is supported by a cord bound to the extremities of the violin (see fig. 7).

recorder to the bridge, which is necessary because of the fairly large forces to be communicated. The recorder was therefore fastened to the top of the bridge by means of a bent strip of metal clamped under the two middle strings, as is shown diagrammatically in *fig. 6*. This arrangement was found to be very satisfactory. When in use the strip of metal which moves with the vibrating armature of the recorder tends to execute a tipping motion whereby a couple is exerted on the bridge in the same direction as by the original movement of the strings. The strings themselves on the loud speaker violin may not of course take part in the vibration, since they are not continually being tuned to the correct pitch by stopping. The motion of the strings is therefore entirely damped by means of a wad of cotton. The strings cannot be omitted, since, by the tension which they communicate to the body of the violin, they affect fundamentally the properties of the latter in its function as organ which determines the timbre [5]).

[5]) The variation in the tension due to the varied stopping during playing is in this respect a second order effect which may be neglected.

The amplification which can be obtained by means of such a loud-speaker violin is of course limited by the above-mentioned non-linear distortion which becomes noticeable at too great amplitudes of the components of the violin. If it is desired to increase the amplification still further, as many more loud-speaker violins as desired must be connected in parallel (*fig. 7* and title photograph).

Let us return for a moment from the laboratory to the concert hall. When the above-described method of amplification is applied the sound of the solo violin is reproduced by five or ten violins at the same time. This raises the question of whether this method might not make it possible to dispense with a large number of musicians in the orchestra. Instead of 25 first violins, could one use a single violinist, and allow 24 other violins to amplify his performance? If the multiple performance of every violin voice had as its only aim an increase in the intensity, this conclusion would in fact be justified. Actually, however, the situation is much more complicated. From the point of view of the composer, without doubt the choral effect

Fig. 7. Series of loud-speaker violins.

of the multiple representation of each voice also plays an important part. This effect is obtained by the slightly differing moment of attack, by the small differences in pitch and in the vibrato, as well as by somewhat differing timbres of the violins and the scattering of the sources of sound over a larger area. The first two of these four factors would be lost if we substituted for the 24 violinists simply 24 loud-speaker violins. It is quite possible that this would be a serious objection. Experience alone can decide the question.

The consideration of the choral effect also however has consequences in the application of the method to the solo violin. The two last mentioned factors — differences in timbre and scattering of the radiating surface — now enter as additional factors in the case of the solo violin, and it is not impossible that the impressions received by the listener will be appreciably altered thereby. Whether the change is permissible, or whether it may even be an improvement, these are questions which cannot be answered by means of laboratory experiments.

INTERESTING LIGHTING EFFECTS OF THE LIEGE WATER EXPOSITION

by L. C. KALFF.

628.974

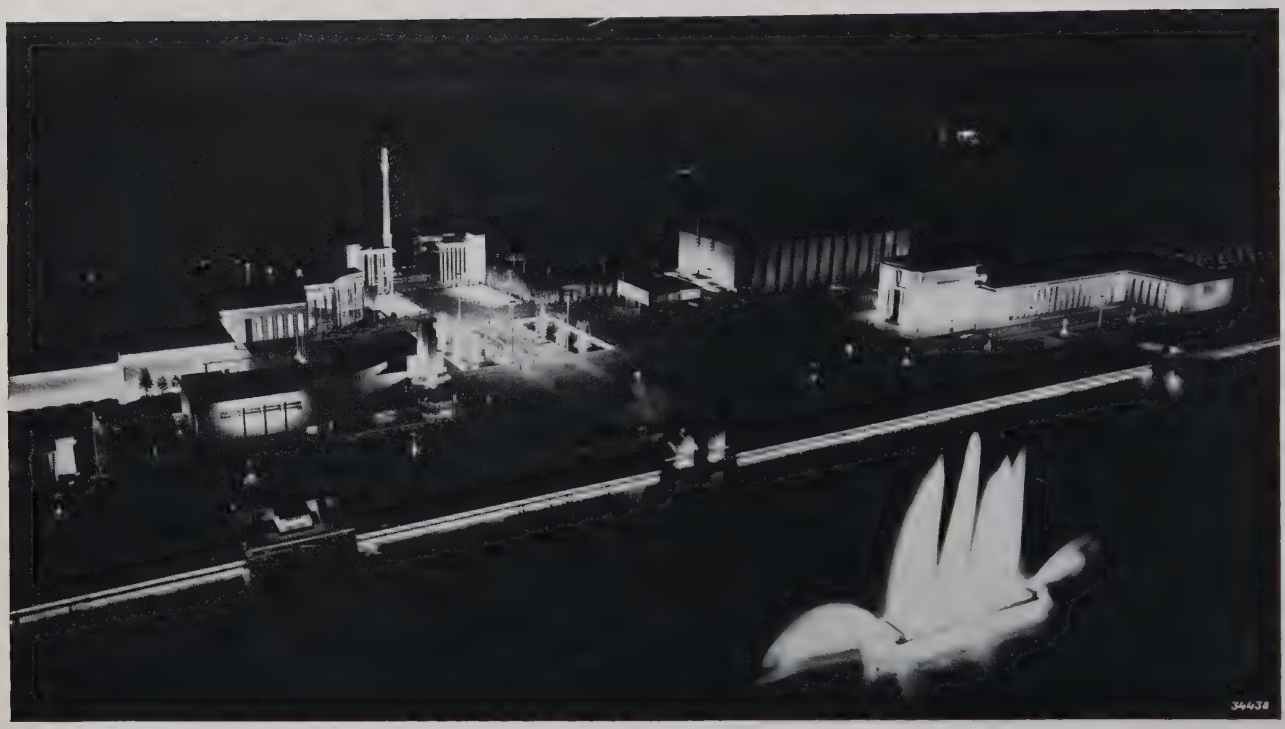

The Liége water exposition, which was opened in 1939, and which was planned primarily to call attention to this busy industry centre of eastern Belgium, was unfortunately compelled by the outbreak of the war to close its gates prematurely. It had already proved a great success, and the attendance and interest of the public were very great. This was undoubtedly due in some part to the logical arrangement which avoided the confusing and fatiguing effect of a too comprehensive world exposition, and to the aesthetically successful building construction under the direction of the young architect Falise.

In planning this exposition the importance of keeping the design and execution as much as possible under a unified direction was immediately understood. A fruitful and interesting coöperation with the Philips consulting bureau for illumination resulted from this conviction.

The grounds of the exposition were laid out on a very generous scale with two permanent boulevards 40 m wide along the banks of the Meuse which is about 180 m wide at this point. The lighting elements had to be in good proportion to these broad open spaces and to the high and massive buildings of the exposition. It is to the credit of the architect that he did not hesitate to accept the unusually large dimensions to which this consideration of proportion led.

In the first place there were the wide boulevards along the Meuse, along which were erected standards 13 m high at distances of 50 m, each bearing six lamps of 300 dlm, which together gave a very uniform illumination of 40 lux over a width of 40 m. The six simple enamelled reflectors in which the lamps were fixed housed in a dome-shaped cap made of eternite (*fig. 1*) in such a way that any one looking along the boulevard was not disturbed by glaring points of light (see *fig. 2*). The standards were manufactured by the Liége steel industry from steel plates bent into circular form and welded. The result was beautifully slender smooth columns which will form part of the permanent lighting system in the future. One of the leading ideas in planning the exposition was the desirability of being able to use the exposition material for practical purposes later on, as well as that of using as far as possible materials (rolled and profile steel,

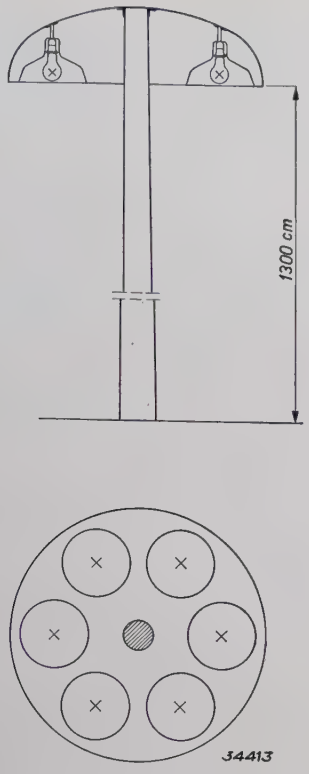

Fig. 1. Construction of the standards for lighting the boulevards along the Meuse. Six 300 dlm lamps are arranged under an eternite dome.

eternite, plates of wood fibre, glass) which could be supplied by the industries in the neighbourhood of Liége.

In order to break the monotony of the main traffic highways a strip of grass was sown along the middle, and lower, more decorative lighting ornaments were placed between the high ones. These lower lamps also provided an extra illumination of the flower beds surrounding them (fig. 2). The ornaments consisted of five m standards crowned by a double cone. The upper cone contained a loud speaker and the lower one three milk-glass globes each containing a 150 dlm lamp. Three arches containing a total of 54 small Argenta lamps shed most of their light upon the flowers. Three strips of netting, painted white, were stretched along the standards and were illuminated from below by three "Cornalux" mirror lamps of 100 watts (for the installation of these lamps see *fig. 3*). As may be seen in fig. 2, these simple motives gave a very pleasing effect, thanks to their correct proportions.

The imposing square directly behind the main entrance, of which the title page photograph gives some impression, was transformed into a water garden. It contained decorative flower mosaics, small fountains, statues and paths. The paths were paved with heavy plates of cast glass lighted from

Fig. 2. Between the stadards for the boulevard lighting, stand the light ornaments for illuminating the flower beds. They are five m high and bear a loud speaker and three milkglass globes each with a 150 dlm lamp. The strips of netting are lighted with "Cornalux" lamps.

below. In contrast with this effect were four enormous standards 20 m high of the same construction as the 13 m standards described above. In this case the eternite cap contained three mercury lamps type NO 2 000 with three ordinary electric lamps of 1 500 watts, which together gave a light source of 13 500 dlm. The centre of the square was in this way very well lighted with an intensity of 60 lux (*fig. 4*).

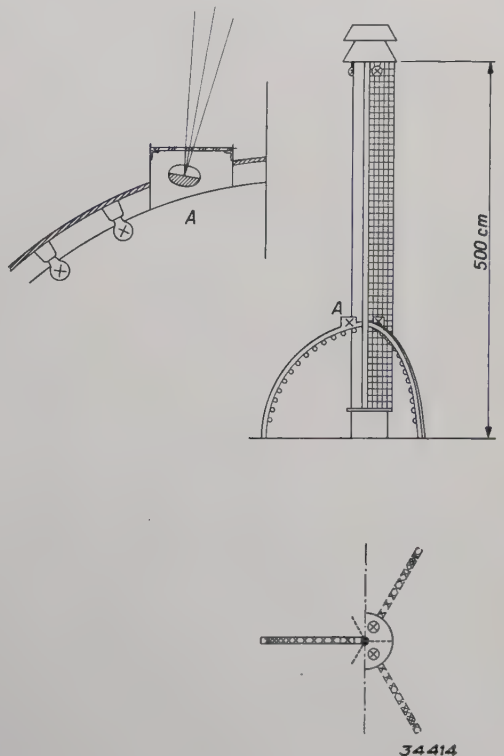

Fig. 3. Construction of one of the ornaments of fig. 2. The detail sketch *A* shows the position of one of the three "Cronalux" lamps illuminating the netting.

The flower mosaic (*fig. 5*) consisted of square flower beds alternating checker-board fashion with square pools of water. At the centre of each pool was a fountain about two m high, which was illuminated at night by means of four "Altrilux" lamps. These are lamps of a special shape and construction (*fig. 6*) intended to be used under water. The bulb is silvered on the inside over half its surface so that a concentrated beam is obtained and a special water-tight reflector is unnecessary. The lamps are cemented into a small cylinder which also contains the lamp socket. The cylinder must be firmly anchored to the bottom of the pool, because, due to the large volume of the lamp, it has a fairly great floating power (± 2 kg). The lamps are placed as near as possible to the surface of the water in

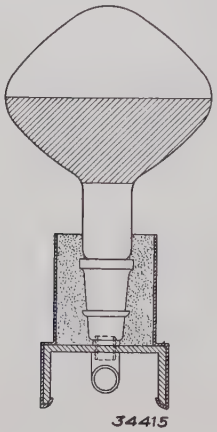

Fig. 6. Construction and assembly of the "Altrilux" under-water lamps.

Fig. 4. The great square behind the entrance is illuminated by four 20 m high standards of construction similar to that in fig. 1. The cap on each standard in this case however contains three mercury lamps, type NO 2000, and three 1500 watt electric lamps, which together give a light flux of 13 500 dlm.

Fig. 5. The flower mosaic of the great square was formed by a checker-board of flower beds and pools. The two m high fountain in each pool was illuminated from below by four "Altrilux" under-water lamps. Each flower bed receives its light from four "Philiflor" reflectors.

order to limit the loss of light, but there must be a layer of water of a certain thickness above the lamp since it would otherwise be broken by the falling water from the fountain. Moreover the high calcium and phosphate content of the water in Liége was a disturbing factor. Within a few days a layer of scale formed on the lamp which was very difficult to remove and which caused considerable loss of light. For that reason the originally planned power of these under-water lamps was doubled

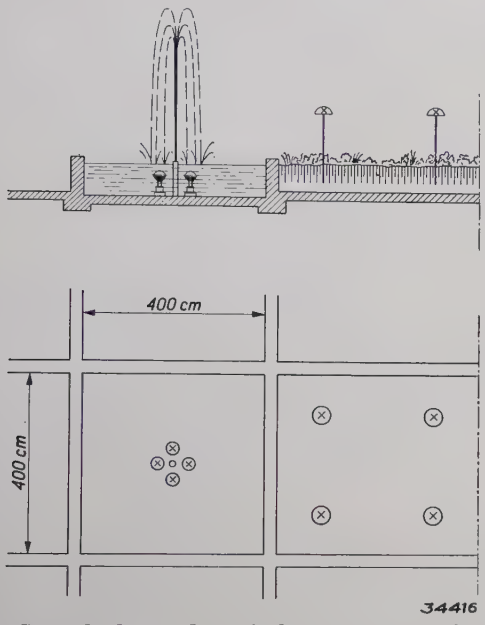

Fig. 7. Ground plan and vertical cross section of a square flower bed and pool.

Each square flower bed was illuminated with four "Philiflor" reflectors with 125 dlm lamps (*fig. 7*).

In the centre of the great square, as may be seen in the title photograph, were two pools and six large statues. These pools were bordered by a sinuous luminous line formed by a row of 40 dlm lamps in an eternite light cove (*fig. 8*). The lamps themselves were invisible but their reflection could always be seen in the water which was kept in continual motion by the play of the fountains. A total of 1 800 lamps were used in this detail. Twelve

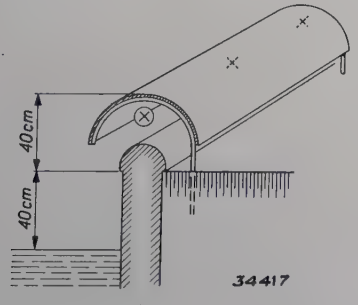

Fig. 8. Construction of the light coves along the pools in the main square. The reflection of the 40 dlm lamps placed in the cove is visible in the water.

Fig. 9. Illumination of the groups of statuary bordering the pools. The sinuous luminous outlining of the pools by means of the light cove can also be seen.

mirror reflectors type FLD with 250 watt searchlight lamps illuminated the groups of statuary (*fig. 9*).

Another interesting part of the illumination of the exposition was formed by the decorations along the 180 m wide Meuse. This broad strip of water had to be incorporated into the illumination so that the exposition should not be cut in two in the evening by the dark strip of water. It is nearly impossible to render a stagnant water surface visible with light sources of limited dimensions, since the water reflects only specularly. Due to the current however the water of the Meuse is in continual motion. Just as the image of the moon is drawn out into a long path of light by a rippling water surface, in the same way a long row of lamps along the bank should transform the whole stream into a brilliant glittering surface for an observer on the opposite bank. Experiments were found to confirm this expectation. Therefore eternite light coves

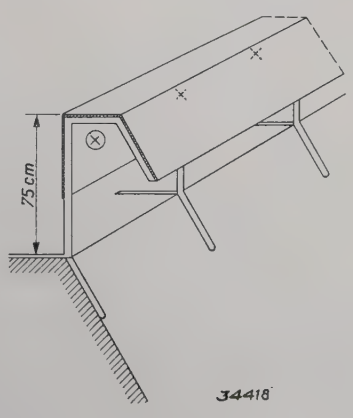

Fig. 10. Construction of the eternite light coves along the banks of the Meuse. The row of 40 dlm lamps in the coves illuminates the stone embankment of the river, and by reflection in the rippling water makes the whole surface of the water visible to an observer on the opposite bank.

Fig. 11. The effect of the illumination along the banks of the Meuse.

(*fig. 10*) $3^1/_2$ km long were set up on both sides of the river, containing 40 dlm lamps at half meter intervals. These lamps illuminated the embankment and together with the lighted buildings were reflected in the rippling surface of the water (*fig. 11*).

It would have been possible to construct numerous illuminated fountains in the river, but it is necessary to keep in mind that the huge dimensions of the water surface would have rendered any ordinary fountain insignificant. It was therefore decided to build a single simple illuminated fountain (*fig. 12*). on a pontoon, but of dimensions in scale with those of the river. The fountain had a jet which could reach 200 m, for which pumps with motors of 1 200 h.p. were necessary. The illumination of this floating fountain was by means of yellow and white light by 64 reflectors with three kW lamps, which were mounted water-tight in the pontoon. Fig. 12 shows another remarkable lighting effect. It was the desire of the architect that there should also be a lighted boundary in an upward direction. For this purpose two flat beams of blueish-white mercury light were projected at a height of 100 m from the top of the mast of the cable railway over the exposition. Due to the scattering by dust particles and mists these fan-shaped beams were visible from below and formed in this way a kind of ceiling over the exposition grounds. The beams were obtained by means of the apparatus shown in *fig. 13*. Two water-cooled super high pressure mercury lamps with a total light flux of 24 000 dlm were mounted in parabolic

Fig. 12. Large fountain in the middle of the Meuse. After dark the fountain is illuminated with yellow and white light.

Fig. 13. By means of two searchlights with a total light flux of 24 000 dlm two broad flat beams of light were projected as a "ceiling" over the exposition.

cylindrical mirrors. The lamps, type SP 2 000, consume only 2.3 kW for a light flux of 12 000 dlm. The beams obtained are very flat and wide (2° in height and 120° in a horizontal direction), and are otherwise quite similar to the beams used to illuminate landing fields in aerodromes (Philips techn. Rev. 4, 93, 1939).

The importance of illumination in the laying out of the exposition is most clearly seen from the fact that a total of 12 000 kW was installed for lighting and 16 000 kW for power. In the middle of July the current consumption was 35 000 k.w.h. per day. Before the premature closing a consumption of 50 000 k.w.h. per day was anticipated for the month of September.

QUANTITATIVE CONSIDERATIONS IN COLOUR PHOTOGRAPHY BY THE ADDITIVE METHOD

by J. F. H. CUSTERS.

535.623 : 771.534.53 : 778.6

The principles and the natural limitations of the photographic reproduction of colours are discussed. On the basis of a fundamentally very simple method of colour reproduction, in which pictures in three colours are projected over one another, the importance for faithful reproduction of a strict linear relation between the amounts of light at the beginning and the end of the whole photographic process is pointed out. The requirement of linearity can be satisfied when the photographic materials used in combination for negative and positive transparency have certain characteristics. In particular it is desirable that the transmission curves of the two materials should be mirror images of each other, as pointed out by Kremer. Various methods are described by which such transmission curves can be realized practically. The methods described have been tested in the Philips Laboratory with different photographic materials, and it has been found that a faithful colour reproduction can be obtained with it for all practical purposes.

Principles of colour photography

When light of two different colours falls simultaneously on the same point of the retina we generally do not observe either of the original colours, but a mixed colour. Spectrally pure red and green, for example, mixed in a certain ratio of illumination intensities on the retina, give together yellow; red and violet together give purple, all the spectral colours together give daylight (white). Experience has shown that it is possible to produce in this way any colour, except some of the spectrally pure colours themselves, by the mixture of other colours. In particular it has been found possible to produce a majority of all existing tints with only three correctly chosen "primary colours" [1]).

This fact forms the basis of almost every method of colour photography. No matter how different the details of the methods may be, they always proceed on the following principle. Three photographs of the object are made in such a way that the transmissibility in each of these pictures is a measure of the amount of light of one of the three primary colours chosen which is observed in the object. In reproduction the three primary colours are remixed in the relation which is determined for every point of the object by the three pictures taken.

Reproduction can be made in two different ways, namely by the "additive" method or the "subtractive" method. If we confine our discussion to reproduction by projection we may describe the two methods as follows. In additive reproduction the three pictures (transparencies) are placed side by side and three coloured light beams each of which passes through only one of the pictures are added together. In the subtractive method the three transparencies which must be coloured in the complementary colours of the three primary colours, are placed one behind another, and the excess light of each primary colour present in a beam of white light is successively removed by the three pictures. This has the same effect on the resulting mixed colour as the addition of the three primary colours. The subtractive method has the advantage that less light is lost in reproduction. This is easily understood when we compare the way in which the impression "white" is brought about in the two methods. In additive reproduction the three coloured light components are obtained by appropriate filtering of the available white light. When this is done and the three light components have to be added together to give "white", only $^1/_3$ at the most (roughly estimated) of the original white light remains. In subtractive reproduction on the other hand "white" occurs when no part of the available white light is removed by any of the three transparencies, and thus the original white light remains quite unweakened.

With this advantage in view the subtractive method has obtained greater practical importance, especially when it is a question of projection in large cinemas where all the available light must be used if the screen is not to appear too dark. Nevertheless the additive method deserves attention since it is simpler in principle and involves fewer possible sources of incorrect reproduction of the colours. In the following discussion we shall confine ourselves to the additive method.

Limitations and conditions of colour photography

For the sake of example we shall examine a method of colour photography which is very simple

[1]) This is explained in detail in the article by P. J. Bouma: The representation of colour sensations in a colour space-diagram or colour triangle, Philips techn. Rev. 2, 39, 1937.

in principle (*fig. 1*). Three filters *a*, *b*, *c* are used each of which has a spectral transmission curve such that upon irradiation with white light the transmitted part of the light is of one of the primary colours, *A*, *B*, *C* (red, green and blue, for instance). Three photographs are made of the object in the usual way with one of the three filters placed before the lens in each case. Three positive transparencies α, β, γ, are made from the three negatives obtained. The transparency α is then projected through the filter *a*, β through *b* and γ through *c*, simultaneously, in such a way that the three pictures coincide on the screen. At each point of the picture a colour mixture occurs which corresponds to the colour of the object.

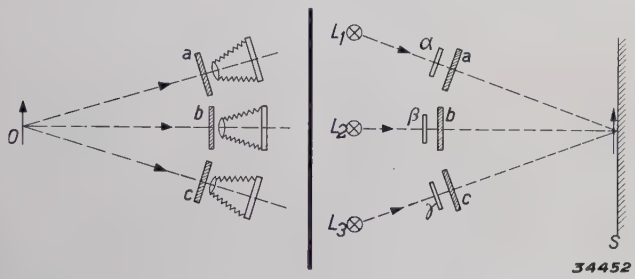

Fig. 1. Diagram of a method of additive colour photography. The object *O* is photographed three times with three filters *a*, *b*, *c* (red, green and blue, for example). Three positive transparencies α β, γ, are then made from the three negatives in the ordinary way. These transparencies are then simultaneously projected on a screen *S* with three sources of white light $L_{1,2,3}$ with the same three filters *a*, *b*, *c*. (For the sake of clarity three cameras are shown here side by side, while actually the three photographs are made one after another with the same camera).

We have been cautious and have used the word "corresponds", because a completely faithful reproduction of all colours cannot be attained in this way. At the beginning of the article we stated that some of the pure spectral colours cannot be produced by mixing. The limitation to which we must submit in this respect can be illustrated by means of the representation of colours in the colour triangle [1]), see *fig. 2*. Each point within the boundaries of the figure represents a tint, and conversely, every tint is represented by a point within this area. The spectral colours lie on the curvilinear boundary. A colour obtained by mixing two colours, lies on the line joining the two colours mixed. With two primary colours, *P* and *Q*, therefore, all the colours can be produced which lie on the line *PQ* in the figure. With three primary colours *ABC* all the colours can be realized which fall within the triangle *ABC*. If a colour lies outside the triangle it means that one of the two ratios of mixing of the primary colours becomes negative, *i.e.* light of one primary colour would have to be used in the mixture in a negative intensity. Since this cannot be done in practice, and since a triangle with three colours at its angles can only include part of the colour area with curved boundaries, it is obvious that some of the colours (very pure colours) fall outside the scope of colour photography with three primary colours.

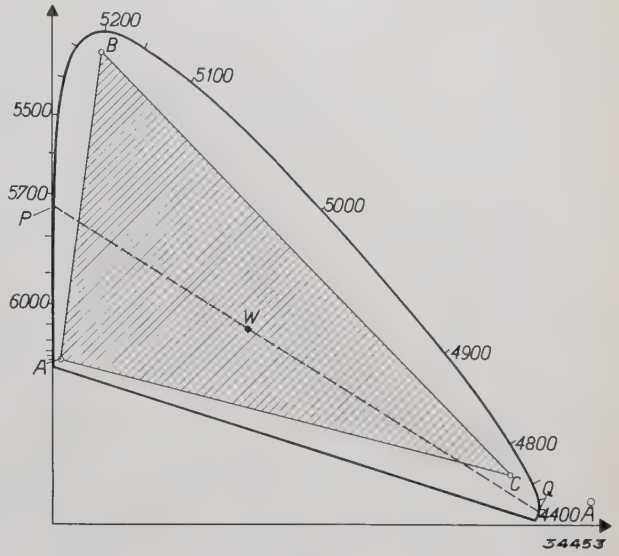

Fig. 2. Colour diagram. Each point represents a tint. The line joining two colours (*P* and *Q* for example) includes all the possible colour mixtures of these two colours. The pure (spectral) colours lie along the curvelinear boundary. With three primary colours, *A*, *B*, *C*, all the colours within the triangle *ABC* can be obtained by mixing. *W* represents white. (By means of the coordinate system indicated the position of each colour can be indicated numerically).

Experience shows that this limitation is not so serious in practice if the primary colours are suitably chosen (namely so that the most important part of the colour diagram is included in the triangle). Even when we have accepted the above-mentioned limitation, we cannot immediately expect that the process of colour photography as here described will result in absolute correspondence between the colour produced and the original colour. In the first place it is not enough that the filters possess the desired primary colours. The same colour can be obtained with entirely different spectral transmission curves of the filters. It has been found [2]) that for a faithful colour reproduction the transmission curve of each filter (combined with the spectral distribution of the light source and the spectral sensitivity curve of the photographic material) must have a very definite shape, derived from the properties of the human eye and the primary colours chosen. The remarkable point in all this is that in the three filter curves calculated negative portions also occur, *i.e.* that the system

[2]) A. C. Hardy and F. L. Wurzburg, Jr., J. Opt. Soc. Am. **127**, 227, 1937.

filter plus photographic emulsion should have a sensitivity less than zero for light of certain wave lengths (see article cited [2])). This can only be realized in a very elaborate way, which is scarcely applicable in practical cases. Approximations of the required filter curves must therefore be accepted, and this is found quite satisfactory in practice.

In the second place, for a faithful reproduction the mixture of the three light components transmitted by the positive must be in the correct proportions for every point of the object. The importance of this condition can again be illustrated by an example. Suppose that the colours P (spectral yellow of about 5700 Å) and Q (spectral blue of about 4470 Å) are mixed in such proportions that the colour W (white) is obtained (see fig. 2). With the help of available experimental data [3]) it is found that upon increase in the intensity of P by only 3.7 per cent a yellow tint is already observed.

The proportions of the three primary colours for a given point of the object can be very simply adjusted to the correct value by suitable adjustment of the light sources in the projection of the three pictures. In order, however, to arrive at the correct proportions for all other points as well, it must be

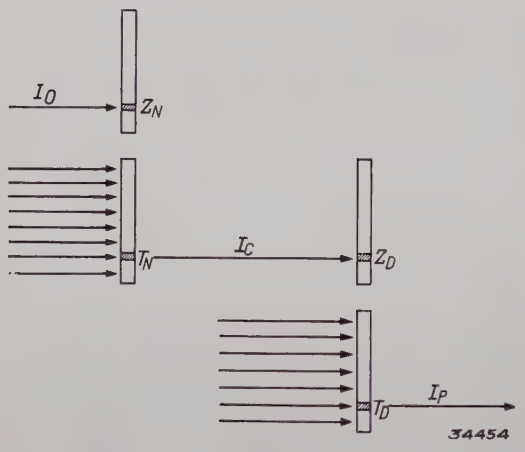

Fig. 3. Upon exposure an amount of light I_O gives a density Z_N (the negative). In copying the fraction T_N of the incident light is transmitted by this point of the negative. Thus the amount of light I_C is incident on the material of the positive transparency and there causes a density Z_D. Upon projection the transparency allows the fraction T_D of the incident light to pass at this point, and the amount of light I_P is incident on the screen.

true of all three transparencies that the amount of light transmitted I_P at every point is proportional to the amount of light I_O which that point received from the corresponding negative when it was photographed.

The way in which this fundamental requirement can be satisfied will be the subject of the following discussion.

Consequences with respect to the density and transmission curves

In order to elucidate the object of the above-mentioned requirement we shall consider in somewhat more detail the process of photographing, copying and projecting (*cf.* the diagrammatic representation *fig. 3*). For the sake of simplicity we shall in the following speak of only one primary colour.

Due to the amount of light I_O which falls on the photographic plate during exposure a density Z_N occurs on the plate (the negative). The density is defined in the following way:

$$Z_N = \lg \frac{1}{T_N} ,$$

where T_N represents the transmission, *i.e.* the fraction of a quantity of incident light which the blackened plate transmits. There exists a relation between Z_N and I_O which is characteristic of the photographic material used [4]), and which is described by a "density curve", in which Z_N is plotted as a function of log I_O, or by a "transmission curve" in which T_N is plotted as a function of I_O. In *fig. 4* the two curves have been drawn for one kind of material. It is characteristic of most density curves that they rise only slowly at small values of I_O (they have a "toe") and then gradually pass on to a longer or shorter straight section, to reach a kind of saturation at high values of I_O.

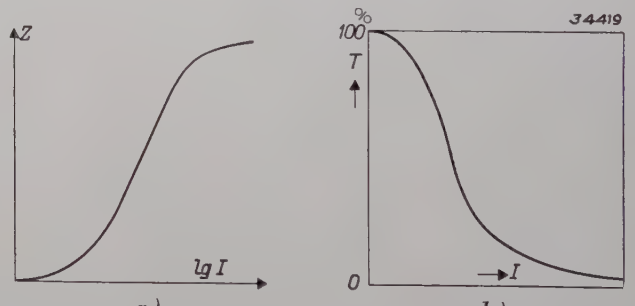

Fig. 4. *a*) Density curve of a photographic material. *b*) Transmission curve.

In copying a negative (see fig. 3 once more), an amount of light I_C falls upon the material used which is proportional to T_N, and which causes a density Z_D (the positive transparency). Z_D is determined by the density curve of the positive

[3]) L. A. Jones and E. M. Lowry, J. Opt. Soc. Amer. **13**, 25, 1926.

[4]) It is assumed that development is always carried out in the same way.

material. In projection an amount of light I_P falls upon the screen which is proportional to the transmission T_D of the positive transparency.

Whether or not the above-formulated condition that

$$I_P \sim I_O \quad \ldots\ldots\ldots \quad (1)$$

is satisfied will obviously depend upon the nature of the two density curves Z_N and Z_D. We shall here examine different forms which satisfy equation (1).

Rectilinear density curves

Let us assume that the two density curves Z_N and Z_D are straight lines, and that Z_N has the slope γ_N and Z_D the slope γ_D. Then the following

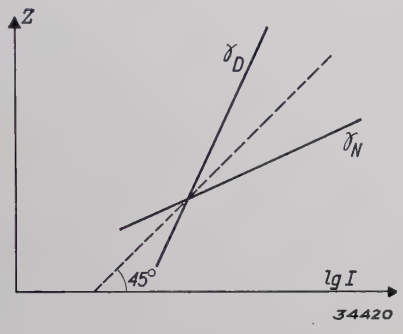

Fig. 5. Two rectilinear density curves for the negative and the positive transparency. The slopes γ_N and γ_D are such that the lines are mirror images of each other with respect to a 45° line.

equations hold where $c_{1,2\ldots}$ represent various constants which are of no importance for our purposes:

$$\lg \frac{1}{T_N} = \gamma_N \lg I_O + c_1,$$

$$\lg \frac{1}{T_D} = \gamma_D \lg I_C + c_2.$$

With the help of $I_C = c_3 T_N$

and $I_P = c_4 T_D$

it follows directly that

$$\lg I_P = \gamma_N \gamma_D \lg I_O + c_5.$$

Equation (1) is therefore satisfied when

$$\gamma_N \gamma_D = 1 \quad \ldots\ldots\ldots \quad (2)$$

This means that the two rectilinear density curves must be each other's mirror images with respect to a line at 45° (*fig. 5*).

In ordinary photography also equation (2), which is called Goldberg's condition, is important when it is a question of faithful reproduction of all the various degrees of brightness. The permissible deviations in that case, however, are considerably greater than in colour photography, since incorrect degrees of dark and light do not so easily give the impression of "unnaturalness" as do incorrect tints of colours.

We have assumed here that the density curves are straight lines. The density curves of most photographic material do indeed possess a longer or shorter rectilinear portion. Equation (2) can therefore be satisfied if only all the light quantities occurring — in photography and in copying — fall within the rectilinear portions. This is however a very unfortunate limitation, especially for colour photography, since it means that small quantities of light which still fall within the toe of the density curve have no effect, while, due to the losses of light in colour photography, it is often just this part of the curve which must be used, and small amounts of one primary colour may have a very great influence on the colour mixture.

Non-rectilinear density curves

It has been found possible to satisfy equation (1) even without a rectilinear density curve. Since the logarithmic representation is mainly used in a density curve because of the simple rectilinear form thereby obtained, if we no longer desire the rectilinear form we can give up the logarithmic representation and use the transmission curve (fig. 4*b*) directly.

In *fig. 6* the transmission curves of a negative and of a positive transparency are given, which in logarithmic representation would not give a straight line, but with which nevertheless a linear reproduction according to equation (1) would be obtained. A definite quantity of light, that which causes the greatest density occcurring, and thus

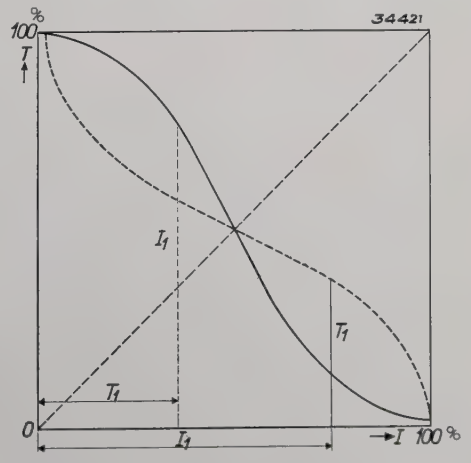

Fig. 6. Transmission curves which are mirror images of each other with respect to the 45° line (full line for the positive transparency and broken line for the negative, for example).

the smallest possible transmission, is set equal to 100 per cent in the figure. In the same way the transmission of an unexposed spot (where there is only fogging) is set equal to 100 per cent. It is characteristic of the two curves that they are mirror images of each other with respect to the 45° line. Thus if an amount of light I_1 causes a transmission T_1, an amount of light numerically equal to T_1 causes a transmission numerically equal to I_1. Equation (1) is therefore satisfied when care is taken that the proportionality factor between I_C and T_N is equal to unity in the process of copying. This amounts to the fact that the amount of light used for copying must be exactly equal to the amount indicated as 100 per cent in the figure.

Is it possible in practice to fulfil the condition mentioned, that the two transmission curves must be mirror images of each other? We have given the full-line curve in fig. 6 a form which is typical of most photographic materials. (The slowly falling first section of the curve corresponds to the toe of the density curve). The broken line curve, its mirror image, has, on the other hand, a form which differs very widely from what is encountered with ordinary emulsions.

The astronomer Dr P. Kremer of Utrecht has suggested an interesting process whereby the mirror image curve can be very approximately realized. Assume that with normal exposure of the negative curve *1* of *fig. 7* is obtained. If the negative is exposed with f times the normal amount of light, a transmission curve of the type 1*a* or 1*b* is obtained, which can be constructed simply by drawing out the section $0 - f \cdot 100\%$ of curve *1*, or compressing it to the abscissa scale 0 - 100%. In the case of curve 1*a*, $f < 1$, the negative is underexposed, the transmission curve is flatter than with normal exposure (*1*). In curve 1*b* $f > 1$, the negative is overexposed, the transmission curve is steeper than with normal exposure. The mirror image of curve *1* (broken line curve) has, however, the property that in the section to the right of the point of intersection with curve *1* it is flatter, and in the section to the left it is steeper than curve *1*, when the extremities in the neighbourhood of $I = 0$ and 100 are disregarded. It is actually found possible to approximate the mirror image curve by means of a combination of an underexposed and an overexposed negative which are copied successively on the same positive transparency. In copying the two negatives a fraction F_1 and F_2, respectively, of the normal amount of light must be used. The required factors f_1 and f_2 for the under and overexposure of the negatives, as well as the factors F_1 and F_2 for the copying can be derived according to Kremer from the shape of the transmission curve *1* by a simple construction. This is explained in *fig. 8* and the text below the figure. The approximation of the mirror image curve obtained by this construction is generally quite good, so that when the positive has the original transmission curve I, the condition for linear reproduction (1) is satisfied in a very wide region of intensities; greater discrepancies occur only at the largest and smallest amounts of light. A certain limitation is laid on the otherwise quite arbitrary shape of the transmission curve I with which we begin, by the permissible amount of error in these regions.

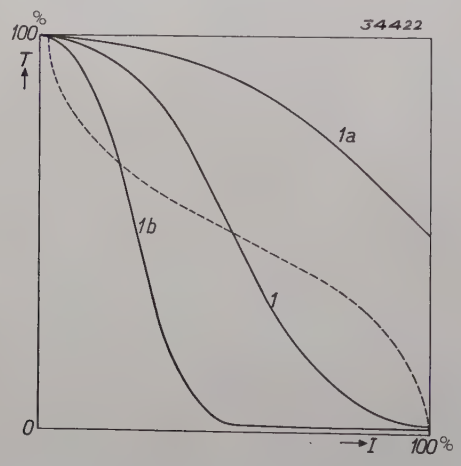

Fig. 7. Transmission curve *1* of the normally exposed negative (its mirror image is indicated as a dotted line). An underexposed negative has the transmission curve *1a* and an overexposed one the curve *1b*.

A series of experiments carried out according to this method in the Philips Laboratory have shown that very good colour reproductions can indeed be obtained. It was found at the same time, however, that in many cases the condition involving the mirror image curves can also be approximated by a simpler device, namely by choosing two suitable emulsions for the negative and positive and pre-exposing one of them with a certain amount of light. The effect of this is demonstrated clearly in *fig. 9*. Fig. 9*a* shows a normal transmission curve; if the whole plate is exposed before the picture is taken (afterward or at the same time is also possible) to the amount of light V the result is fogging corresponding to the point A, and there remains only the portion A-B of the transmission curve for further variations (fig. 9*b*). If this section is plotted anew with abscissae and ordinates from 0 to 100 per cent it represents a new transmission curve as shown in fig. 9*c*. With a suitably chosen value of V it is possible to make this transmission curve the mirror image of another (given) emulsion.

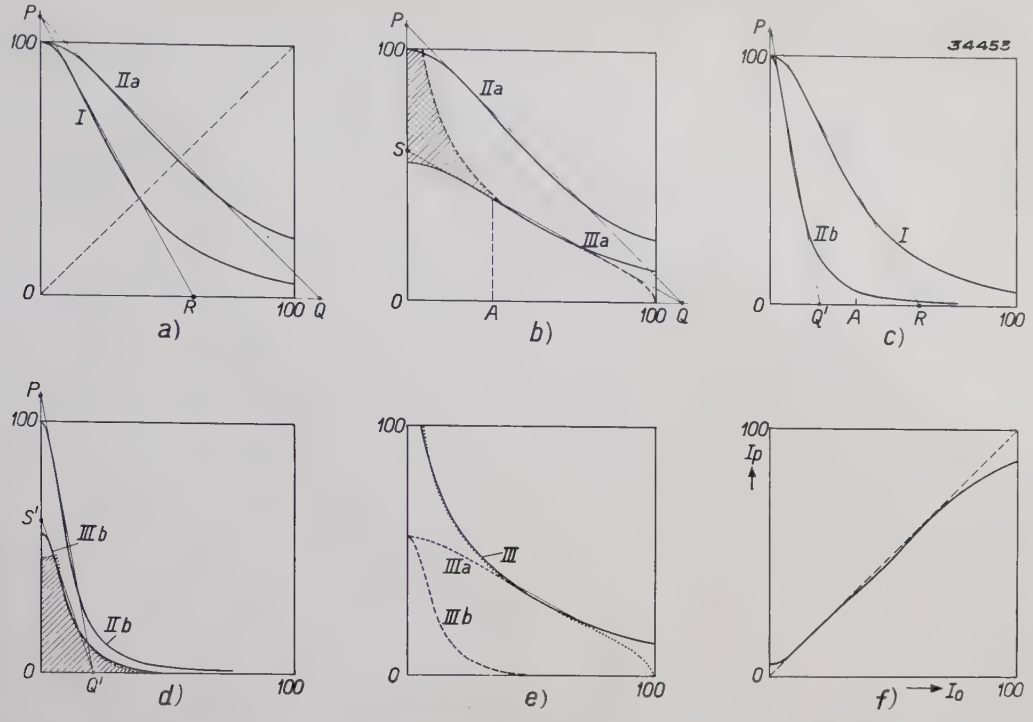

Fig. 8. *a*) Curve *I* is the normal transmission curve of the material to be used for negative and positive transparency. A large part of the curve is approximately a straight line, as indicated, which cuts the axes at *P* and *R*. If *OQ* is drawn equal to *OP*, then $f_1 = OR/OQ$, the factor for the underexposure of the first negative which then attains the transmission curve *IIa*.

b) In copying the underexposed negative with the normal amount of light (100%) the ordinates of *IIa* would indicate the amounts of light incident on the positive. What is however desired is the amounts of the dotted line (mirror image of curve *I*). Therefore only the fraction F_1 of the normal amount of light is used for copying, so that one is concerned as it were with transmission curve *IIIa* when $F_1 = OS/OP$. In the construction here given $F_1 = f_1$. The left-hand portion of *IIIa* is too low and would have to be completed by the shaded portion.

c) For this purpose the overexposed negative is used. The factor $f_2 = OR/OQ'$ for overexposure is so chosen that the negative transmits practically no light from the point *A* on the abscissa, from which point *IIIa* is a sufficiently close approximation of the mirror image curve.

d) The required fraction F_2 for copying the overexposed negative is found by plotting the part of the mirror image curve to be completed (shaded area of *b*), and approximating it by a straight line *Q'S'*. Then $F_2 = OS'/OP$ and the apparent transmission curve *IIIb* is obtained.

e) In the successive copying of the two negatives on one positive transparency, the same total amount of light is incident on the latter as if only one negative with the transmission curve *III* were used; *III* is the sum of *IIIa* and *IIIb* and approaches the desired mirror image curve of *I* (dotted line) very satisfactorily. The relation between I_P and I_O which is finally obtained is represented in

f) The 45° line represents the ideal case.

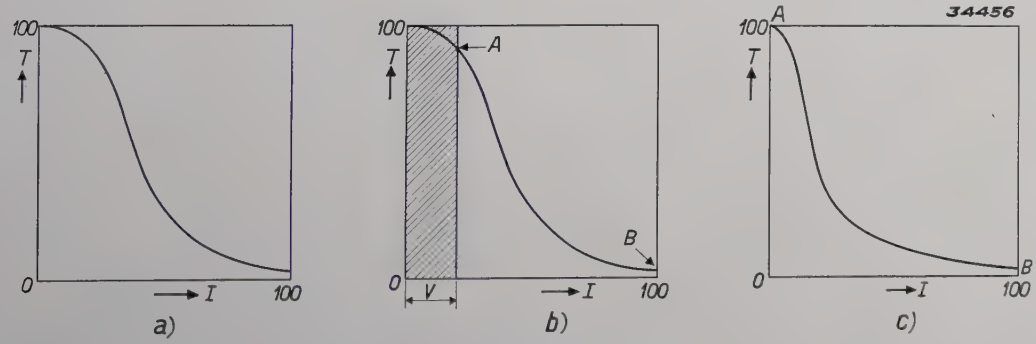

Fig. 9. By pre-exposure with a suitably chosen amount of light *V* (*b*) the nature of the transmission curve of a photographic material can be influenced in a definite way (*c*), so, for example, that it becomes the mirror image of the curve of another given material.

In *fig. 10* an example is given which was obtained in the experiments under consideration. It may be seen that a satisfactory approximation of the linear relation between I_P and I_O has been obtained by this simple method.

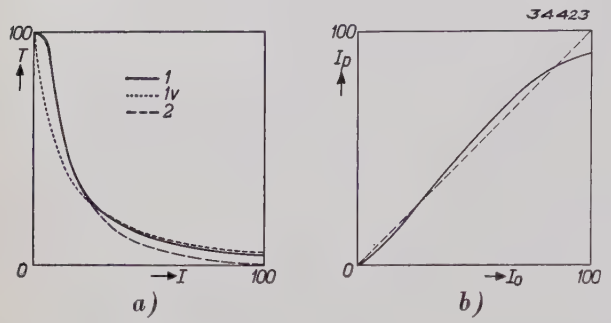

Fig. 10.*a*) The transmission curve *1* of the negative material is changed by pre-exposure into the curve *1 v* which is a close approximation of the mirror image of the transmission curve *2* of the positive material.
b) The ratio obtained between I_P and I_O.

In conclusion it may be pointed out that a special case of this condition involving mirror images occurs when a transmission curve is given which is symmetrical with respect to the 45° line. The curve is then at the same time its own mirror image and the material can therefore be used for both negative and positive. In our experiments we actually found certain emulsions among the usual kinds which possess approximately such a transmission curve, and with which therefore it is sufficient to secure accurate dosage of the amounts of light in photographing and copying in order to obtain satisfactorily linear reproduction. With certain materials symmetry of the transmission curve could be achieved by appropriate pre-exposure; in that case the pre-exposure must of course be applied not only in the case of the negative but also in that of the positive.

THE ELECTROMETER TRIODE AND ITS APPLICATIONS

by H. van SUCHTELEN.

621.317.723 : 621.385.3

Since the anode current of a triode can be influenced by a change in voltage of the control grid when there is no current flow in the grid circuit, a triode is in principle suitable for electrostatic measurements of potential. In this article the characteristics and the possibilities of application are discussed of the electrometer triode, type 4 060, which was designed especially for this purpose.

In many physical and electrotechnical experiments the problem is encountered of measuring the voltage of sources of voltage which possess a very high internal resistance. It is of course essential that the voltage meter used should consume as little current as possible, so that the terminals voltage measured will remain equal to the EMF of the source.

Very small currents also are sometimes measured by sending them through a high resistance and then measuring the voltage across the resistance. In such cases also a voltage meter with a high resistance is called for, since the meter shunts the measuring resistance, and thus limits the magnitude of the total resistance to be applied, thereby also limiting the sensitivity of the circuit.

In such cases an electrometer is best used whose deflection is caused by the electrostatic action of charges, and which in principle therefore consumes no current at all.

The electrometer in its different types (quadrant electrometer, string electrometer, etc.) is a fairly expensive and delicate instrument, so that its possibilities of application are limited. A much sturdier arrangement can be obtained by replacing the electrometer by a triode which also allows a currentless measurement of the voltage. The anode current can be influenced by voltage variations of the control grid without any current flowing through the grid circuit.

The term currentless must in this case be taken with a grain of salt. As is generally known a grid current immediately occurs when the grid becomes positive with respect to the cathode. This can, however, easily be avoided by a correct circuit arrangement, but even when the grid potential is negative a small current often remains which may be due to various causes.

In the first place, in the "pinch" of an ordinary radio valve, *i.e.* in the glass holder of the various electrodes, there will be a certain leakage between the grid and one of the other electrodes. This weak leakage current is permissible in ordinary radio and amplifier connections, but it is usually not

permissible when a triode is used as electrometer.

In the second place, it is inevitable that a vacuum tube, instead of being an absolute vacuum, contains a small residue of gas. If gas molecules are ionized by the anode current the positive ions are drawn toward the electrode with the lowest potential, *i.e.* the control grid, and neutralized. This amounts to a grid current.

In the third place the control grid may have a certain thermionic emission, because it is fairly strongly heated by the glowing cathode, and moreover in some cases it becomes covered in spots with a highly emissive material, due to the evaporation of the surface of the cathode. Besides the thermionic emission there may also be photoelectric emission due to light incident from the outside and to soft X-rays which come from the anode bombarded by electrons.

The total grid current which occurs as a result of the various causes here mentioned is less than 0.1 microampere in ordinary amplifier valves. For certain electrometrical applications the degree of insulation of the control grid found in these valves is sufficient without further measures being taken. In order however to satisfy the much higher requirements which are made in certain cases, a special electrometer triode has been constructed in which measures have been taken to make the grid current considerably smaller.

Construction of the electrometer triode

In *fig. 1* the construction of the Philips electrometer triode, type 4 060, is shown. The grid is fastened to two long glass rods in order to make the path of creeping currents as long as possible. In order to make this arrangement possible, control grid and anode have different positions than is usual in amplifier triodes; they are situated on opposite sides of the filament. Both the electrodes are flat plates. The wire lead of the grid is fused through the glass at the top of the bulb, thus as far as possible away from the lead-in of the other electrodes. When the outside of the bulb is well cleaned and dry the leakage current over the glass of the supports and the bulb may be neglected.

From the point of view of thermionic emission also, this placing of the control grid is more satisfactory than the ordinary arrangement, because the temperature of the grid is kept lower due to the great heat radiation of the flat plate. It will usually be unnecessary to take special precautions against photoelectric emission because the shielding from external electric fields which is usually present will give sufficient shielding against the light as well. The illumination of the grid by the glowing cathode is avoided by using an oxide cathode which emits at a very low temperature.

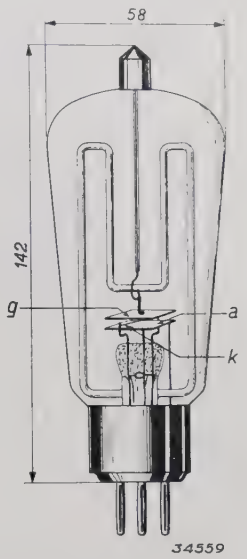

Fig. 1. Construction of the electrometer triode, type 4 060. The control grid is mounted on long glass rods; the lead-in of the grid is fused in through the top of the bulb. Very good insulation is obtained in this way.

Finally, considerable decrease in the grid current caused by ions and X-rays is obtained by choosing a very low anode voltage, namely 6 volts. At this voltage no ions are yet formed, because the energy which an electron obtains in passing through a potential difference of 6 volts is not enough to ionize an atom of the gas, while the X-rays excited at this voltage are much weaker than at the usual anode voltages of about 250 volts.

The result of these precautions is expressed in the valve characteristic reproduced in *fig. 2*. It may be seen that the total grid current becomes practically zero when the anode current is zero. From this it may be concluded that the leakage current over the glass may be neglected compared with the currents connected with the anode current. With normal grid voltages the grid current is of the order of 10^{-15} A, *i.e.* at least 10^6 times as small as may be expected in valves of the ordinary type [1]).

The other characteristics of the electrometer triode, type 4 060, are given below:

Heating voltage	about 0.7 V	Specific values for every tube are given in the instructions.
Heating current	about 0.6 A	
Anode voltage	max. 6 V	
Slope	25 μA/V	
Amplification factor	1	
Grid current	$< 10^{-14}$ A.	

[1]) To give some idea of the size of this current, it may be stated that it corresponds to 6 000 electrons per second.

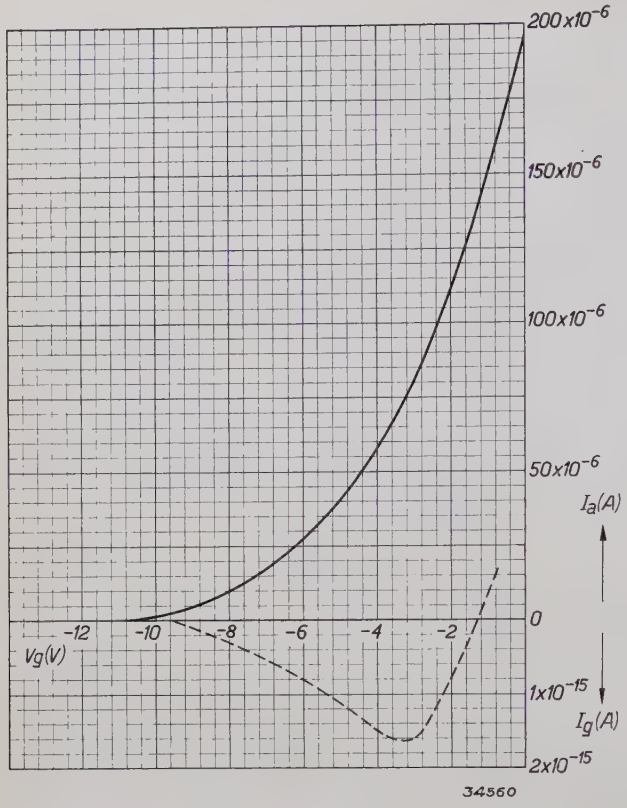

Fig. 2. Grid current and anode current as functions of the grid voltage for an anode-voltage of 4 V. At negative grid voltages the grid current is smaller than 10^{-14} A. For a certain grid voltage the grid current is exactly zero.

Connections of the electrometer triode

In most of its connections the electrometer triode is used as a zero indicator. The voltage to be measured is compensated by a variable counter voltage which can be read off. Both voltages are connected in series in the grid circuit of the electrometer triode. If there is an excess voltage due to insufficient compensation, this is manifested in the anode current. The compensation can therefore be adjusted using the reading of the anode current as indicator.

This method has two advantages. In the first place the form of the characteristic, anode current as a function of the grid voltage, plays no part. The required value follows from a direct reading of the compensation voltage, and the slope of the valve affects only the accuracy with which the compensation can be regulated.

In the second place, the actual voltage on the grid always retains about the same value, independent of the voltage measured. Arrangements can therefore be made so that one always works at a voltage at which no grid current flows (fig. 2), and at which therefore the measurement is entirely electrostatic in character.

A fairly general scheme for the measurement of voltages by the compensation method is indicated in *fig. 3*. The grid voltage V_g is adjusted approximately at the value at which no grid current flows. This value can be determined empirically in the following way. When the grid of the triode is entirely insulated, it automatically assumes the potential in question. If it did not originally have that potential, electrons will flow to it or away from it until the potential is reached at which the current becomes zero, and then the situation becomes stationary. In fig. 3 the switch is set at the insulated middle position S_1, and the grid then takes on the required potential. The corresponding anode current is then read off, and with S at the lowest position, V_g is so adjusted that the same anode current is again obtained.

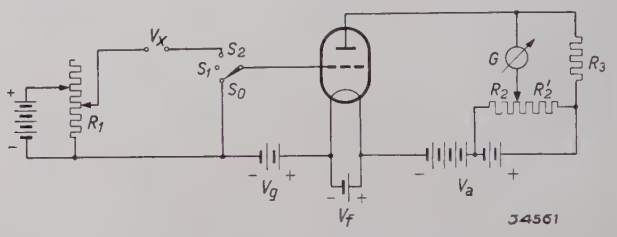

Fig. 3. Circuit for the comparison of a voltage to be measured with an accurately known compensation voltage (from R_1). The galvanometer is in the so-called currentless connection, *i.e.* the potentiometer R_2. R_2 is so adjusted that the galvanometer indicates zero when the voltage applied to the grid, other than V_g, is zero. This is the case when the grid switch is set on S_0, or when the correct compensation has been obtained (with the grid switch on S_2).

On the extreme left may be seen the compensation voltage tapped off from the resistance R_1, in series with the voltage V_x to be measured. The point on R_1 where it is tapped off must be so adjusted during the measurement that the anode current does not change when the switch S is moved from the lowest to the highest position. V_x is then equal to the compensation voltage used, which is known from the part of the resistance R_1 tapped off, through which an accurately known current flows. As a rule this arrangement is calibrated by connecting a standard element in place of the voltage V_x to be measured.

In order to be able to read off very small current variation, as is necessary for accurate compensation, a connection is used in the anode circuit in which the normal anode current does not pass through the galvanometer. The anode current flows through the resistance R_3, and there causes a certain voltage drop, so that the voltage on the anode is lower than that of the anode battery. At the lowest terminal of the galvanometer G, by means of an adjustable tap on the potentiometer R_2, the same voltage R'_2 can be applied so that G carries no current. If however the anode current

changes, the equilibrium is disturbed, and a current flows through the galvanometer. If the internal resistance of the galvanometer and potentiometer is sufficiently small compared with R_3, this current is practically equal to the change in the anode current. Thus the entire scale is available for the measurement of the current fluctuations, and one may choose as sensitive a galvanometer as desired without taking into account the normal anode current.

The measurement is now carried out as follows. The switch is first set in position S_0, and the potentiometer R_2 so adjusted that the current through the galvanometer is zero. When one now switches over to S_2, a deflection of the galvanometer will generally occur. Potentiometer R_1 is then adjusted so that this deflection disappears.

Since the slope of the electrometer triode is 25 μA/V an error of 1 mV in the compensation voltage will cause an anode current variation of 0.025 μA, a value which can be registered with a relatively simple instruments. In practice however the accuracy is determined not only by the sensitivity of the galvanometer, but also by the stability of the circuit arrangement. When, for example due to a fluctuation in the temperature of the cathode, the anode current changes slightly, the equilibrium of the galvanometer connections is upset. This drift can cause an error of several hundredths of a volt in the measurement of the compensation voltage, and is therefore much more important than the error caused by the limitation of the sensitivity of the galvanometer. Fortunately the drift generally takes place very gradually, so that it is of little importance when the measurements in position S_0 and that in position S_2 are carried out in quick enough succession.

The drift would however be disturbing when a series of measurements had to be carried out, for instance of a voltage which itself slowly varies. One would then be compelled by the drift to note the zero position of the galvanometer each time anew, or to adjust it to the same value.

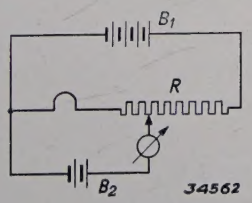

Fig. 4. Connections for the purpose of keeping the voltage of the heating current battery constant. The filament is fed by the battery B_1; the battery B_2 is made currentless by adjusting the potentiometer R. If however the voltage of B_1 changes, the missing portion is supplied by B_2. Since B_2 is very lightly loaded its voltage is quite constant.

Since the drift is caused mainly by fluctuations in the heating current, considerable improvement can be obtained by very carefully keeping the voltage of the heating current constant. A simple connection making this possible is given in *fig. 4* and explained in the text beneath.

In connections in which the electrometer triode does not serve as a zero instrument, but as an actual meter, the problem of fluctuation is still more important. In such a case the effect of any voltage fluctuations can be eliminated to a large degree by using the arrangement reproduced in *fig. 5* [2]). These connections, used here for measuring a photocurrent, are so arranged that any fluctuations of battery voltage do not lead to a change in the current through the galvanometer, because upon such fluctuations the potential of both connections of the galvanometer change by the same amount.

The circuit has two identical electrometer triodes whose cathodes are connected in parallel. The voltage drop V_x to be measured is applied to the grid of the first electrometer triode. The galvanometer is connected in the anode circuit of this electrometer triode in a manner corresponding in principle with fig. 3, except that the resistance R_2' is replaced by the internal resistance of the second electrometer triode.

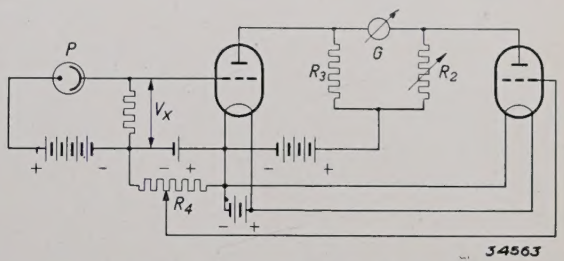

Fig. 5. Symmetrical connections of two electrometer triodes. If a voltage V_x acts between the terminals the galvanometer G shows a deflection. Variations of the battery voltages have equal effects in both the anode circuits, so that they do not cause a deflection of the galvanometer.

By means of the potentiometer R_4 the grid voltage of the second valve is so adjusted that the two valves have about the same anode current in the absence of the measuring voltage [3]). By fine regulation of the resistance R_2 (which corresponds approximately with R_3) the galvanometer is finally rendered currentless.

The two valves now function under practically the same conditions. They have the same battery for the heating current, the grid voltage and the

---

[2]) J. F. H. Custers, Z. techn. Phys. **14**, 153, 1933.

[3]) In order to do this when the triodes differ slightly, one takes as second triode the one which has a slightly lower anode current at a given grid voltage.

anode voltage. If a change occurs in one of the battery voltages it has the same effect on both valves, and it is very probable that the two anode currents will remain alike, and therefore also that the galvanometer will remain currentless. Only when a measuring current is applied to the first valve is the equilibrium upset and G shows a deflection.

The fluctuation is reduced to about one tenth by the use of these connections.

Applications of the electrometer triode

As already stated the electrometer triode can be used in general in every setup in which an electrometer would otherwise be used. There are however several types of measurements in which in the course of time the electrometer triode has won special recognition. We shall deal with them separately.

p_H measurements

The quantity p_H is a measure of the concentration of hydrogen ion c in a solution, $p_H = -\lg c$. Measurements of p_H are repeatedly made in chemical laboratories, in the testing of foods and farm products, in medical research, etc.

The commonest method of measuring p_H makes use of the fact that the potential of special electrodes immersed in the solution changes proportionally with p_H. Among the various electrodes which exhibit this property, the most suitable is the so-called glass electrode. Besides certain advantages, however, this electrode has the less desirable property that its internal resistance is very high, namely of the order of 10^7 ohms.

In order to determine the EMF of a source of voltage with this high internal resistance, an electrostatic method of measurement is indicated. The compensation circuit arrangement reproduced in fig. 3 is usually employed with an electrolytic cell with a glass electrode in the place of V_x. If the potential is measured accurately to within 1 mV, the value of p_H is determined with an accuracy of 1.7 hundredths of a unit [4]), which is more than adequate for most practical purposes.

A sensitivity of 1 mV can easily be attained, as explained above. If we examine to what extent the result of the measurement could be influenced by the residual grid current, we find that it is quite unnecessary to have the electrometer triode work at an especially favourable point; the maximum grid current is less than 10^{-14} A within a large range of grid voltages, and with this current a voltage loss of only $^1/_{10\,000}$ mV would occur at an electrode with an internal resistance of 10^4 ohms.

Radiation measurements with the ionization chamber

The intensity of radioactive radiation can be measured by determining its ionizing action. In most cases the ions formed by the radiation are collected on a very well insulated condenser whose voltage varies with the time. Since one is here concerned with extremely small charges it is here again important that the voltage meter should consume practically no current. Since the electrometer triode consumes a current of less than 10^{-14} A, an ion current of 10^{-12} A can be measured with an accuracy of 1 per cent.

A current of 10^{-12} A corresponds to a radioactivity of the order of 10^{-9} Curie, which may be considered very weak. If the same instrument is used to measure X-rays, with a sufficiently sensitive ionization chamber a current of 10^{-12} A corresponds to such a low radiation intensity that it cannot be made visible by means of a fluorescent screen. In both cases therefore the grid current of the electrometer triode has no bad effects, so that it is unnecessary to choose the working point such that the grid current is exactly zero.

In another important application of the ionization chamber, namely for the measurement of cosmic rays, the attainable ion currents are much smaller, of the order of 10^{-14} A. In this case the grid current at a given adjustment of the grid voltage cannot in general be neglected. According to a method indicated by Prof. Clay [5]), however, the grid current can be kept practically at zero during the measurement.

The method has also been used in this laboratory for the measurement of very weak photocurrents, and has been described in detail in this periodical [6]). In the circuit given the photocell can immediately be replaced by an ionization chamber.

As stated previously all of these measurements can also be made with an ordinary electrometer, and the advantage of the electrometer triode lies especially in the great sturdiness of the apparatus. In the measurements by Clay referred to some of the experiments were carried out on board ship, and the ionization chamber with the electrometer triode was even lowered overboard to a considerable depth below the surface.

[4]) The potential of a glass electrode at room temperature varies -0.058 volts per unit of p_H. A change in the potential of 1 mV thus corresponds to a change in p_H of 0.017 units, which means that the hydrogen ion concentration changes by 4 per cent.

[5]) J. Clay, Physica **4**, 124 and 654, 1937.

[6]) P. M. van Alphen, Philips techn. Rev. **4**, 71, 1939.

The measurement of photocurrents

A photocell gives a current which is proportional to the incident light flux, and which amounts for instance to 20 or 30 microamperes per lumen. In certain measurements the light flux becomes so small that special devices must be used in order to be able to measure the photocurrent. This is the case for example in the photometry of stars or of lines in the spectrum [7]).

It is possible to carry out the measurement of the photocurrent in the same way as the measurement of the current through an ionization chamber in which the voltage on a condenser is determined when the condenser is charged by the current. As to the connections, we refer to the article cited in footnote [6]), in which the precautions are also discussed which must be taken in order to obtain a sufficiently high insulation and satisfactory shielding at all sensitive spots.

If the currents are not extremely small, but of the order of 10^{-13} A, for example, a simpler method may be used. Liquid resistances of the order of 10^9 to 10^{10} ohms may be made up. Currents which are just too small for direct measurement with a galvanometer (10^{-10} to 10^{-11} A) give voltages of the order of 0.1 V over such resistances. Since, as we have seen, the electrometer triode makes possible voltage measurement with an accuracy of 1 mV, a sensitivity of 10^{-13} to 10^{-14} A is obtained in this way. This is also about the limit of sensitivity set by the residual grid currents.

[7]) A star of first magnitude gives an illumination intensity of 10^{-6} lux. If, for example, the telescope has a lens (or mirror) of 40 cm diameter one obtains a light flux of 10^{-7} lumen. Such a small light flux, and even smaller ones, also occur in the spectral photometry of sources of light. See in this connection the article cited in footnote [6]).

ABSTRACTS OF RECENT SCIENTIFIC PUBLICATIONS OF THE N.V. PHILIPS GLOEILAMPENFABRIEKEN

1438: J. Sack: Forces acting during the transfer of material through the welding arc (Weld. Industr. **7**, 234-240, July 1939).

For the contents of this lecture held before the Institute of Welding in London the reader is referred to: Philips techn. Rev. **4**, 9, 1939.

We take the opportunity at this point to draw attention to an inaccuracy in the article referred to. For the theoretical estimation of the kinetic energy with which the drop is thrown off the welding rod, it is of some concern at what length of *radius of the neck of te drop* the moving force of electrodynamic nature is in equilibrium with the total sum of the opposing forces, and not with the weight of the drop alone. This consideration is developed further in the above-mentioned lecture, with as result that the electrodynamic forces are found to contribute only very little to the total energy. The mechanism of the transfer of the weld material may therefore be summed up in the following way. *The electrodynamic forces cause the constriction at the neck of the drop and the drop is then thrown off by the explosive forces.*

1439: F. A. Kröger: Some optical properties of zinc silicate phosphors (Physica **6**, 764-778, Aug. 1939).

Zinc silicate phosphors and zinc beryllium silicate phosphors activated with manganese are mixed crystals of zinc silicate and zinc beryllium silicate with manganese silicate. Mixed crystals with from 0 to 50 molecules per cent of manganese emit two bands at 25° and —180° C with maxima at 5 200 and 6 100 Å. The emission bands of zinc silicate-manganese phosphors are caused by electron jumps in the bivalent manganese. The 0 to 50% mixed crystals of zinc and manganese silicate absorb light in three different wave-length ranges. The first absorption range also exists with pure zinc silicate and must be considered as a crystal absorption. The second absorption range only appears when manganese is present but it also has the properties of a crystal absorption. In the third absorption range we are concerned with a band system; each band corresponds to a definite electron transition in the ion Mn^{++}. Upon irradiation with light from each of these absorption regions luminescence occurs in the emission bands characteristic of the bivalent manganese ion. Upon irradiation with wave lengths of the two regions of crystal absorption phosphorescence and fluorescence occur together, while irradiation with the manganese absorption bands gives only fluorescence.

1440: F. A. Kröger: Fundamental absorption of ZnS-MnS and ZnS-CdS-MnS mixed crystals (Physica **6**, 779-784, Aug. 1939).

Zinc sulphide possesses a fundamental absorption region with a long-wave limit at about 3 380 Å.

When manganese sulphide is taken up in the lattice a new absorption band appears with its edge at 3 650 Å. This band is similar to the fundamental absorption band found with manganese sulphide. When cadmium sulphide is taken up by zinc sulphide-manganese phosphors the fundamental absorption region of the zinc sulphide is shifted toward the red of the spectrum.

1441: J. L. Snoek: Magnetic after-effects at higher inductions (Physica **6**, 797-805, Aug. 1939).

Continuing with the investigations described in **1339** and **1399** on magnetic after-effect phenomena, a sample of pure iron was prepared, with which, by the addition of very small amounts of carbon homogeneously dispersed, an extremely strong magnetic after-effect could be observed. The magnetic after-effect with stronger fields was studied on this sample. Since it followed from the investigations with weaker magnetic fields that the permeability and the magnetic field were not the most important quantities, but the reciprocal of the permeability and the magnetic induction B, all the experimental data were recalculated for these latter quantities. The relative intensity of the after-effect remains constant to $B = 6$ gauss, and falls at $B = 100$ gauss to about 10% of the original intensity. This follows from the curves which indicate the manner in which the reciprocal of the permeability depends upon the temperature, and also from its behaviour at low temperatures and high inductions. It is remarkable that a demagnetization, at which the induction is 100 gauss at the most, results in no appreciable decrease in the reciprocal of the permeability at the same temperatures. Much higher inductions are required for this, for instance up to 10 000 gauss. The substance thus has a tendency to return to the old state of magnetization after demagnetization.

1442: H. Bruining and J. H. de Boer: Secondary electron emission, part IV. Compounds with a high capacity for secondary emission (Physica **6**, 823-833, Aug. 1939).

A pure compound of an alkali metal has a higher secondary emission than the metal itself. It is further described how the electrons, which are bound to the atoms of the electronegative element in the highest occupied energy band have the greatest chance of being emitted as secondary electrons. It is shown that it is impossible that all the secondary electrons should come from the metal atoms within or on the surface of the compound. These metal atoms provide only the conduction electrons.

1443: H. Bruining and J. H. de Boer: Secondary electron emission, part V. The mechanism of secondary electron emission (Physica **6**, 834-839, Aug. 1939).

On the basis of a simple energy scheme it is easily understood that the compounds of metals with a low ionization energy, which consist of ions with closed electron shells, can give a high secondary emission, while the compounds of metals with a high ionization energy must exhibit a relatively low secondary emission.

1444: J. A. M. van Liempt and W. van Wijk: The rare gas content of air dissolved in water (Chem. Wbld. **36**, 555, Aug. 1939). Original in Dutch language.

Air dissolved in water contains about twice as much of the rare gases as is present in the ordinary atmosphere.

1445: A. Claassen: The volumetric and quantitative determination of zirconium and hafnium single and together with selenious acid (Z. anal. Chem. **117**, 252-261, Aug. 1939). Original in German Language.

When zirconium and hafnium solutions are heated for some time with an excess of selenious acid, the initially formed insoluble basic selenite passes over into a crystallized compound of the composition $Zr(SeO_3)_2$ and $Hf(SeO_3)_2$ respectively.

Since these compounds have exactly the composition expressed by the formula, they are useful for the quantitative determination of zirconium and hafnium. For the volumetric determination the precipitate is dissolved in sodium fluoride and sulphuric acid and the selenious acid form is determined iodimetrically. In the case of zirconium correct results are obtained in this way, but with hafnium the results are from 1.0 to 1.4% too high. For the gravimetric determination the precipitate is dried at 120 to 200° C and then weighed. Since small amounts of selenium precipitate out, the results are often somewhat too high. By converting a known amount of a mixture of ZrO_2 and HfO_2 into the selenite, and determining the selenious acid radical volumetrically, the content of hafnium can be determined with an accuracy of about 1%.